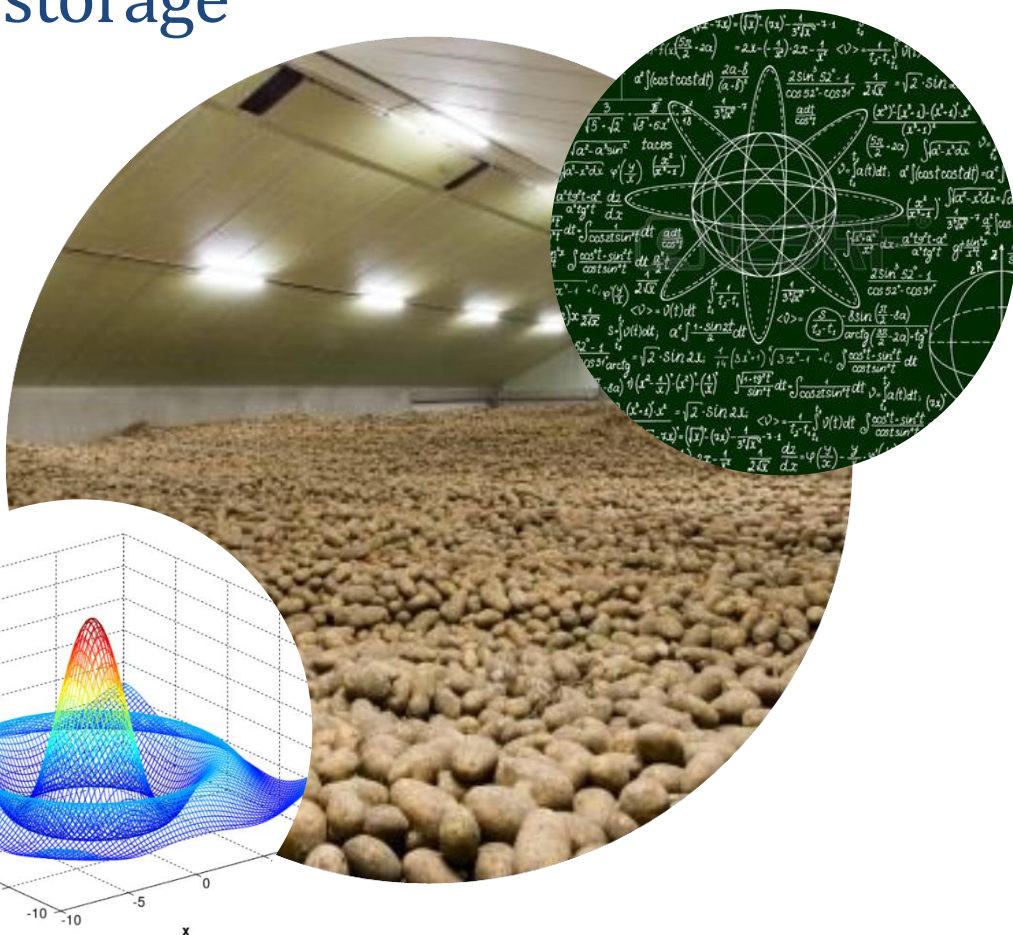


Modelling the physiological changes of the potato skin regarding water loss during long term storage

Stefan Hol

940809353120

February 2018



WAGENINGEN
UNIVERSITY & RESEARCH

OMNIVENT
Experience innovation.



Modelling the physiological changes of the potato skin regarding water loss during long term storage

Name course : MSc Thesis Biobased Chemistry and Technology
Number : BCT-80436
Study load : 36 ects
Date : February 2018

Student : Stefan (SJE) Hol
Registration number : 940809353120
Study programme : MBT
Report number : 068BCT
Supervisor(s) : Nik Grubben
Examiners : Karel Keesman, Gerard van Willigenburg
Group : Biobased Chemistry and Technology
Address : Bornse Weiland 9
6708 WG Wageningen
The Netherlands

Abstract

Water loss is one of the major problem in the potato storage industry. It especially effects the income of farmers, as it influences the two factors determining the potato price: the quality and the weight of the potatoes. Therefore, the present work was undertaken to develop new storage strategies minimizing water loss, thus the processes involved in water loss was investigated. In this research, the moisture transfer coefficient of the potato skin was determined over time. This coefficient is the ratio of the water diffusion coefficient of the skin over the thickness of the skin. This skin moisture transfer coefficient has a big influence on the rate of water loss.

In this research, a 1D computational fluid dynamics (CFD) model is proposed, to simulate the skin moisture transfer coefficient over time, using real storage data. From analysis it appeared that the skin moisture transfer coefficient is increasing over time, meaning that the ratio of the diffusion coefficient over the skin thickness increases. Therefore, the diffusion coefficient becomes larger.

Preface

This report is the result of my research done during my MSc thesis at the Biobased Chemistry and Technology group (BCT) of Wageningen UR. During this thesis I have worked on modelling the physiological changes of the potato skin regarding water loss during long term storage.

I have learned a lot about simulation techniques and overcoming challenges that occurred in modelling with real data. Of course I received help.

First of all I would like to thank my supervisor Nik Grubben for giving me the opportunity to join his project. Likewise for his supervision and tips.

Furthermore I would like to thank Karel Keesman & Rachel van Ooteghem for their advices and comments. It was really helpful to speak with people with a so much knowledge of the theory, by which I was remembered to think of the theory when facing problems instead of thinking about things within the project.

A big thank you to Ellen Slegers, Lars Kiewidt, Costas Nikiforidis and the thesis ring students, who helped with improving my writing skills and for feedback on the project.

I also would like to thank Sander Bezuijen, Frank van Gool, Gerard Hegemans, Frank de Pont, Tycho van Noorden and Rien Wesselink of the COMSOL multiphysics helpdesk. They answered a lot of questions regarding the software and helped me debug.

Of course I would like to thank the team in BCT, PhDs, students and technicians for their advices, help and for the pleasant time. For all the other people who gave comments, helped me somewhere in the process or just put me back to the positive flow when facing problems, thank you.

Stefan Hol

Wageningen, February 2018

Contents

1	Introduction.....	1
1.1	Background.....	1
1.2	Problem statement.....	1
1.3	Research goals.....	2
1.4	Approach	2
1.5	Outline thesis.....	2
2	Theory.....	3
2.1	Potato growth and harvest.....	3
2.2	Potato storage	3
2.2.1	Quality loss during storage.....	4
2.2.2	Curing conditions.....	5
2.2.3	Wound healing	5
2.3	Lenticels.....	6
3	Modelling potato water loss	7
3.1	Membrane diffusion model.....	7
3.2	Moisture diffusion model.....	8
3.3	1D moisture diffusion model.....	9
4	Simulating the skin moisture transfer coefficient	12
4.1	Materials.....	12
4.2	Parameters, variables and assumptions.....	12
4.3	Model evaluations	15
4.4	Model calibration	16
5	Discussion & recommendations.....	23
6	Conclusion	26
7	References.....	27
	Appendices	33
	Appendix A Membrane diffusion model.....	34
	Appendix B 3D moisture diffusion model.....	37
	Appendix C Deciding on the air domain size for the 1D moisture diffusion model	40
	Appendix D Deciding on the potato thickness in the 1D moisture diffusion model	41
	Appendix E Deciding on the flow regime for the 3D moisture diffusion model	42
	Appendix F Deciding on the air domain size for the 3D moisture diffusion model	47
	Appendix G Results of the calibration experiment	49

1 Introduction

1.1 Background

Potatoes (*Solanum tuberosum*) are a food crop originating from the Andes. They have been consumed for more than 8000 years (Popenoe et al., 1989). In 2014 approximately 385 million tonnes of potatoes were harvested worldwide (FAO 2014) which makes it the 8th highest produced food crop in the world. Although the potato originates from South America most potatoes are produced within Asia and Europe. According to FAOSTAT 2014 data The Netherlands are the 6th producing country of Europe and the 10th of the world with 7.1 million tonnes. Most produced potatoes are destined for human consumption. Most potatoes are harvested in a short period in late summer or early autumn. As 7.1 million tonnes of potatoes cannot be consumed at once, potatoes are stored have to be stored after harvest.

To maintain the potato quality during storage, optimal storage conditions are preferred. Optimal storage conditions are realised experimentally (Driskill et al., 2007) and with use of global models (Xu & Burfoot, 1999). Within these global models the effect of most physiological processes in the potato are unknown or not taken into account during the optimization of the storage climate.

Some of the changes during storage were already noticed a long time ago, like sucrose (Singh & Mathur, 1937), reducing sugars, nitrogen, protein, ascorbic acid, and dry matter content (Blenkinsop et al., 2002). The effect of variety, temperature and humidity on weight loss and respiration in storage was studied (Butchbaker et al., 1973). A low temperature (6-10°C), high humidity (approximately 96%) storage performed best (Firman & Allen 2007). Although the information on the physical and physiological behaviour of the potato, it is not captured over time in models.

An important physical process is the water loss of the potato. Water loss has effect on the quality development and enhance disease spreading during storage (Singh & Kaur 2016). For example, pressure bruised potatoes loose up to 3 times more water than good quality potatoes (Lulai et al., 1996). Moreover, potatoes are sold on the weight of the potatoes times a quality factor. As potatoes consists of approximately 80% water (USDA National Nutrient Database for Standard Reference) the weight and quality loss has a big influence on the profit.

The main barrier to water loss is the skin of the potato (Riederer & Schreiber, 2001). The skin is a structure consisting of multiple layers. During storage the skin can change in chemical composition, structure or thickness. This changes will influence the water loss. Knowing how this changes can result in new storage strategies to decrease the water loss. To determine how the skin changes models can be used.

1.2 Problem statement

In the model of Grubben & Keesman (2015), the water loss of the potato is modelled with 2 constant factors for the evaporation and the respiration. In this thesis will be focused on a time dependent rate of water loss, to investigate if this would improve the model of Grubben & Keesman.

1.3 Research goals

In this research first the most relevant physiological processes involved in water loss and skin development in storage will be investigated. When these processes are known a model will be created to determine the changes of the physiological parameters over time. This model will be validated by data from other years or other storage facilities then the ones used for creating the model. These steps are performed to determine:

How do biological, physiological and physical changes within the potato skin are influencing the water loss of the potato during long term storage.

This results in the following research questions:

- Which biological, physiological and physical changes occur within the potato regarding long term storage?
- How can the change of the skin moisture transfer coefficient of the potato skin during storage be captured in a spatially distributed model?
- How does the skin moisture transfer coefficient of the potato skin change during storage?

1.4 Approach

First a literature study was performed on the causes of water loss and its consequence for the potato quality. A model describing the physical process of water loss will be described. The skin moisture transfer coefficient will be estimated using the model, weight loss and climate data from an Omnivent storage facility. It is commonly accepted in agriculture (Peters & Wiltshire, 2002) that the skin gets thicker during storage. However it is also possible that the chemical composition of the skin changes. Both these physiological changes of the skin are expected to reduce the water loss. It is already known that the water loss changes over time during storage. However not how the physical and physiological parameters, like the diffusion coefficient and the thickness of the skin, change. These changes are of interest when aiming to minimize the water loss of the potatoes. Therefore, the changes of the moisture transfer coefficient of the potato skin is investigated. The model is calibrated for one specific potato variety and validated by data from another storage facility, the same facility but a different year or another potato variety. New storage strategies to increase quality after storage and maximize profit, by minimizing water loss, can be investigated with this model.

1.5 Outline thesis

First short information on potato growth, harvest and storage will be given (chapter 2). Followed by information regarding quality and physiological processes influencing this quality during storage (chapter 2.2). The most important process will be modeled, in chapter 3 the model will be described and discussed. Afterwards the results of the simulations will be shown and discussed (chapter 4). Followed by a reflection on the work performed during this thesis (chapter 5).

2 Theory

In this chapter, farm practice steps relating to the potato, from sowing until the end of the storage period, are discussed. The storage period will be discussed in more detail, including processes and potato characteristics which can influence the storage period. This information will provide insight in the processes and farm practice steps most important regarding potato quality. It is general assumed that the water concentration within the potato is the main aspect for the quality. When this is confirmed or disproved, the specific parameters relating the most important processes are determined and will be modelled in chapter 3.

2.1 Potato growth and harvest

Potatoes have a vegetative reproduction. Therefore, first potatoes of the same desired variety are sowed, so-called seed potatoes. In the farm practices for consumption and seed potatoes many differences can be distinguished. For consumption potatoes the quality standards are a species specific starch and sugar content, depending on application, and a lack of diseases. However, for seed potatoes the quality standards are based the potential of the potato to sprout, seed size and also lack of diseases (van Loon, 2007). A diseased seed potato will result in contaminated soil and therewith a partly infected field. Therefore, these potatoes are not allowed as seed (UNECE, 2016). Small tubers produce more stems per weight than large tubers (van Loon et al., 1993), on these stems new potatoes will grow. During growing season the farm practice is aimed to reach the best possible product, the quality of the product in the field will determine the start quality of the potatoes in storage and is therefore very important.

A few weeks before harvest, the green parts of the plants are removed. Nowadays all steps, from sowing to harvesting, are performed mechanically. Harvesters separate potatoes from the leftover green parts, soil, clods and stones using rollers and webs, during this processes potatoes can become damaged (Firman & Allen, 2007).

2.2 Potato storage

After harvesting, the potatoes are stored in bulk or in bins as they cannot be sowed or consumed immediately. In bulk storage the potatoes are all on top of each other in a large pile. This pile can be up to 3-5 m high. In contrast to this, in bin storage boxes or bags are used to stack the potatoes. The advantage of bin storage, compared with bulk storage, is the possibility to stack to greater heights. Heights of 7.5 meters are used by some farmers, this reduces the amount of floor surface needed. This greater height is possible as less pressure is on the potatoes since this pressure is only coming from the other potatoes in the box or the potatoes in the bags on the same plateau (Pinhero et al., 2009). Using bins also facilitates the use of a single storage facility for several varieties of potatoes or even other crops. These crops or varieties need to have the same storage conditions to store them together. In bin storage the temperature, relative humidity and atmospheric composition control is more difficult and the equipment and utilities more expensive (Pinhero et al., 2009). In the Netherlands where most farmers have lots of acres with the same species, bulk storage is the main applied system. For bulk storage climate models and control systems are developed, for example Xu & Burfoot (1999), Grubben & Keesman (2015), Grubben & Keesman (In press). For bin storage other models are made for the climate control (Chourasia & Goswami 2008; 2007a, b, c, d; 2006 a, b, c; Chourasia et al., 1999; Chourasia et al., 2004; Chourasia et al., 2005; Chourasia et al., 2006).

2.2.1 Quality loss during storage

During storage the potatoes lose approximately 4% of its water in large scale storage (Heltoft et al., 2016, Veerman & Wustman 2005) and 2% in small scale storage (Heltoft et al., 2016, Öztürk & Polat 2016). This water loss is due to evaporation of water through the skin and 10-50 % respiration (Butchbaker et al., 1973), due to processes within the potato, which causes shrinkage, pressure bruising (Lulai et al., 1996) and weight loss of the potato (Kilpatrick et al., 1955, Secor & Gudmestad 1999). Moreover, quality loss can be caused by pressure bruising due to the stacking of the potatoes and damage by other organisms, like rodents and micro-organisms, all strengthened by water loss. During the whole storage period the quality of the potato, initially determined by the farm practice and the climate, changes. To minimise these changes specific storage strategies are used, like the specific storage climate conditions in the first weeks.

Halfway through the last century experiments were performed on the specific effect of storage temperature on the weight loss (Hardenburg, 1949). In these days no anti-sprouting agent was used and therefore, sprouting was taken into account next to the water loss. Nowadays, anti-sprouting agents like chlorpropham, maleic hydrazide, ethylene, carvone and spearmint oil (CTGB, toelatingen bank) are permitted to use in the Netherlands. When using non-resistant potatoes and potatoes without internal sprouting (Sawyer & Dallyn 1964) and the chlorpropham added at the correct time and dose, the weight loss is only due to the water loss. The use of correct time and dose of the anti-sprouting agent is assumed during this thesis.

Water loss can also result in bruising and blue/black discoloration, greater peeling losses, reduction of culinary quality, all leading to economic loss (Singh & Kaur 2016). The skin is the physical barrier for water and weight loss, however, limited information can be found in literature. Potatoes with larger skin cuts have a higher moisture loss than potatoes with little or no injury (Sparks 1954). Similar results were found investigating weight loss in combination with damage index (Misener 1994). The damage index is a system to quantify the damage of a potato. Vogt et al. (1983) found a changing water permeability over time. As a changing water permeability means a change in the rate of water loss, it is worthwhile to look into the skin characteristics and development to determine how this change happens. When the processes resulting in the change of water permeability are known, new storage strategies to minimize water loss can be found.

Next to the water loss, microbial infections can occur during storage. Infections of bacteria and fungi will spread extensively under favourable conditions in the storage. Late blight and pink-rot that already occurred in the field continues during post-harvest storage. Blight is caused by the *Phytophthora* fungi (Singh & Kaur, 2016). Damaged potatoes can suffer from dry rot, watery wound rot and other infections. But also other diseases such as powdery scab, black scurf, and silver scurf are possible on potatoes (Singh & Kaur, 2016). Due to these diseases, the potatoes lose water more quickly (Daniels-Lake et al., 2014). 70% of the damage to potatoes is caused during harvesting, 30% during transport and storage (Kleinschmidt & Thornton, 1991). It is worthwhile to take a look at damage prevention during harvest (Rady & Soliman, 2013) and possible recovery of the potato during storage. Damage is reduced during harvest by regulating speed of the harvester and corresponding equipment and their material choice (Bentini et al., 2006; Firman & Allen, 2007). However, both damaged and undamaged potatoes will go into storage. Already in 1978, it was found that inoculation occurs before the storage, as microbial infected soil is in the wounds (Adams & Griffith 1978). Therefore, the skin thickness and quality is important for quality of the potatoes and the water loss.

2.2.2 Curing conditions

One of the first periods during storage is the curing period, during this time the wounds on the potato are healed. Only this period of storage is optimized to minimize the water loss, although the potato is losing water during the whole storage period. This results in changes within the skin as a new layer of skin is formed, this process will be discussed more in chapter 2.2.3. The effect of a curing period on the total weight loss of a potato during 4 month storage was determined (Schipper 1971). With high relative humidity and relatively high temperatures (7.5-20°C) during the first 2 weeks (the curing period) the weight loss was between 4.8-5.9% of the original weight. Using a lower relative humidity the weight loss was between 5.1-7.0%. Without the 2 week curing conditions the weight loss was 6.8-7.5%. Thus the curing period has a lowering effect on the long term weight loss.

Moreover, the quality of the potato skin has nutritious effects. For example, immature potatoes show a big loss of vitamin C during the curing stage (first weeks) while mature tubers, with a better developed skin, show almost no loss (Panitkin et al., 1979). The least loss over a time period of 5 months is found with overall storage at 5°C (Effmert et al., 1961). Although some conditions and physiological changes within the potato or on the potato skin are known it is not quantified depending on storage conditions.

2.2.3 Wound healing

During the curing period wounds are healed, but also the microbes in already infected wounds are activated. Wound healing is a complex process known on a cellular level (Sabba & Lulai, 2002). Next to this, the complete metabolic pathway of the production of suberin is known (Bernards, 2002) as other of the skin molecules (Lulai, 2007). Suberin is one of the main molecules in the new potato skin (Serra et al., 2014). This knowledge is not yet adapted in storage strategies. Optimisation of the storage strategies to increase wound healing speed could improve the quality of the potatoes and decrease the spreading of the diseases.

On a wounded potato a replacement phellem is formed, in which the number of layers of cells is higher than in the original one. The phellem is a sort of cork layer and consists of multiple layers of dead cells and waxes, and provides the barrier for water and gas transfer. However, the new barrier is after a month still less effective by approximately a factor 100 compared to the original skin (Schreiber et al., 2005). This means that the plant compensates by adding more and more insufficient layers (Lendzian, 2006). Although suberin and other waterproof waxes were present in a quantity of 60% of the normal periderm.

In the first days after wounding the water permeability decreased and suberin and wax production increased. Afterwards the content of suberin and waxes continued to rise, however, the permeability became stable. This means that the presence of suberin and other waxes does not give an almost perfect barrier to water loss (Schreiber et al., 2005). Also no clear correlation between these components and the water permeability was found.

The water permeability of the potato skin when they are in the soil is a factor 3.3 – 25 higher than when harvested and placed in storage. A steady state of this permeability decrease was reached after 2 weeks. Within these experiments from Schreiber (et al., 2005) the temperature and relative humidity did not influence the decrease in permeability when placing the potatoes in storage (During 2 months of storage of the potatoes the phellem thickness increased 10 to 15 percent. The thickness is

complicated to determine. However, the easier to determine dry weight of the skin can also be used (Groh et al., 2002).

2.3 Lenticels

All above-ground organs, like leaves, stems, flowers, fruits and glands, of potatoes are coated by an extracellular layer (Riederer & Muller, 2008): the cuticle. This is a barrier against water loss (Riederer & Schreiber, 2001). The water permeability represents the barrier properties of the cuticle (Schönherr & Ziegler 1980; Groh et al., 2002).

In potatoes the periderm is believed to act in a similar way to the cuticle–epidermis–stomata complex in other plants (Lendzian, 2006). This complex and periderm are both a sort of skin. This cuticle–epidermis–stomata complex is responsible for the regulated exchange of water and gasses with the environment. The periderm consists of the phellogen, the phelloderm and the phellem. The phellem is interspersed with lenticels. Lenticels are raised pores in the stem of a woody plant and are paths for water oxygen and CO₂ exchange. The transport properties of phellem and lenticels can be characterized for different plant species if the type of diffusant, driving forces, temperature, water content, and presence or absence of lenticels is controlled (Lendzian, 2006). The water permeance of five different tree species phellem decreased linearly with increasing phellem thickness (Groh et al., 2002).

Lenticels are also present on the phellem of the potato. Lenticels are the only sites where gas exchange occurs and moreover possible entry points for several microbial pathogens to the potatoes (Adams 1975). Lenticels may often become bigger in wet soils, whereas in dry soils a suberin based layer can form. This layer lowers the permeability of lenticels to gases and the susceptibility to pathogens (Hooker 1981). For example the fungi, *Oospora pustulans*, responsible for skin spot enters via the lenticels (Allen, 1957) also the bacteria, *Erwinia carotovora*, for blackleg disease (Scott et al., 1996). However, the common dry rot fungi, *Fusarium*, is only able to enter at damaged skin (Bojanowski et al., 2013). Phellem with and without lenticels from various types of trees and plants were compared for their permeances (Schönherr and Ziegler 1980; Groh et al., 2002). They concluded that lenticel areas were somewhere between 6 and 40 times more permeable than the surrounding phellem. Lipids within the phellem seemed not to be involved in controlling the diffusion of water and gases through the lenticels (Lendzian, 2006). However, it has been reported that a waxy layer covers the entire inner surface of lenticels (Park, 1991) to prevent liquid water from entering the lenticel. It is unknown if this waxy layer is the suberin based layer described by Hooker (1981). Due to this waxy layer lenticels remain accessible for gas exchange even during rain.

A lot of the mentioned processes regarding loss of quality are based or affected by the amount of water and/or the water loss. Water loss, mainly caused by evaporation and respiration can result in bruising, discoloration, peeling losses, and worse culinary quality. Therefore, the water loss can be seen as the most important process and is chosen to be modeled. The process of water loss is influenced by the skin characteristics, like thickness, the presence of lenticels and wounds. Currently, only the first period of storage is optimized to minimize the water loss, by optimizing the wound healing process, although the potato is losing water during the whole storage period. To optimize the whole storage period, the skin thickness and the moisture diffusion coefficient of the skin are the specific parameters chosen to be modelled, since both are influencing the rate of moisture loss through the skin. To improve the potato quality the rate of moisture loss should be limited.

3 Modelling potato water loss

The loss of quality and mainly water content has a major impact on the income of farmers, as it influences the two factors determining the potato price: the quality and the weight of the potatoes. Therefore, the water loss from the potato has to be determined. Curing conditions and wound healing were not taken into account, as no data or equations on these processes was found. The same holds for the other quality aspects mentioned in chapter 2.2.1.

To determine the water loss from the potato, a membrane diffusion model was defined. This model simulates the rate of moisture loss through the skin of the potato over time. In this model, the assumption was made that the water is homogeneously distributed over the potato. This means the concentration of water near the skin is the same as everywhere else in the potato. To check the validity of this assumption, a computational fluid dynamics (CFD) model was made which includes the water transport within the potato, the moisture conductivity. To limit computation time a 1D CFD model was made, called the 1D moisture diffusion model. When the 1D moisture diffusion model does not disprove the assumption of a nearly homogeneously distributed water concentration within the potato, the membrane diffusion model can be used. Subsequently from this 1D model a 3D CFD model was made, the results of the 3D model are shown instead of the 1D pictures, when more descriptive pictures are useful to visual phenomena.

3.1 Membrane diffusion model

The skin of the potato can be seen as a membrane, with the flesh of the potato on one side of the membrane, and the air on the other side. Lenticels on the skin of the potato are not taken into account. In the potato storage air is moving with a certain speed across the surface of the potato. In both the potato, potato skin and the air is a certain concentration of water. Depending on the skin characteristics and the water concentrations the water flux can be determined. A model to determine the relative humidity and the temperature of the air in the storage for each position in time is present (Grubben & Keesman in press). A schematic overview of membrane diffusion is shown in Figure 1, with the inner side of the potato as the feed and the skin as the membrane, in the right part of Figure 1.

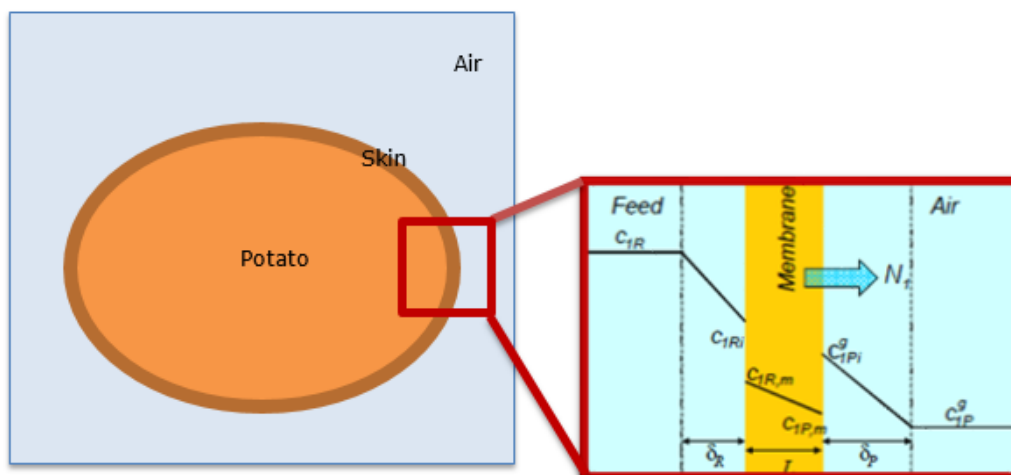


Figure 1 schematic overview of membrane diffusion (Janssen 2014). In the right part of the picture the potato is represented as the feed and the skin as the membrane. C_{1R} is the concentration in the potato and C_{1P}^g the concentration in the air. C_{1Ri} & C_{1Pi}^g the concentrations at the interfaces and $C_{1R,m}$ & $C_{1P,m}$ the concentrations on the interfaces in the skin.

The rate of water transport at a specific time and spot (N) ($\frac{kg}{m^2s}$) through the skin is based on a resistance: the skin moisture transfer coefficient (kov), and a driving force ($C_p - C_r$) ($mol\ m^{-3}$), in the following relationship:

$$N = -kov(C_p - C_r) \quad (3-1)$$

In which the skin moisture transfer coefficient, is determined by the moisture diffusion coefficient of the skin over the thickness of the skin.

$$kov = \frac{D_{skin}}{d_{skin}} (m\ s^{-1}) \quad (3-2)$$

3.2 Moisture diffusion model

To determine the influence of the moisture conductivity, simulations were performed. The water loss of the potato (the concentration change) ($\frac{\partial c_p}{\partial t}$), the moisture conductivity of the potato (D_p) and the skin moisture transfer coefficient (kov) are included. To investigate the influence of the moisture conductivity, a moisture diffusion model is set up. When the moisture conductivity does not affect the spreading of water through the potato in a way which disproves a nearly homogenous concentration of water within the potato, the membrane diffusion model (Appendix A) can be used. A schematic overview of the 3D CFD-model can be found in Figure 2. Within this system heat and water transfer between the air and potato takes place. Besides, air flows through the system. Two domains are taken into account, the air domain (Ω_a) and the product or potato domain (Ω_p). The air flow is described by the black arrows.

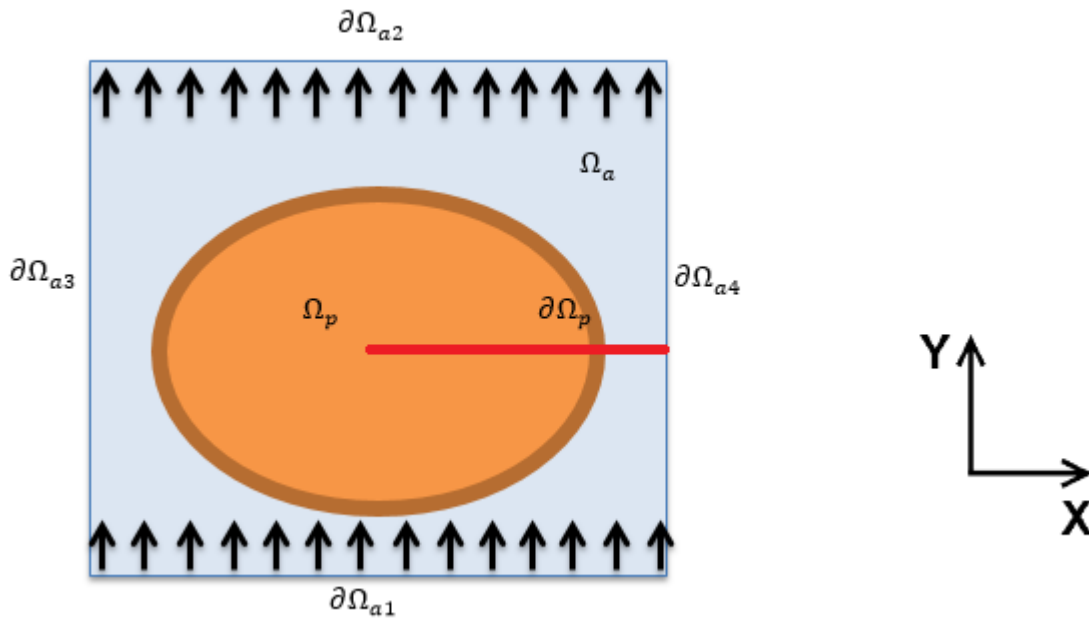


Figure 2 schematic 2D overview of the 3D moisture conductivity model

3.3 1D moisture diffusion model

First a 1D model is described, secondly a 3D model was created (Appendix B). The 1D model is faster and is the most basic representation of reality, making orientating simulations relatively simple. Within a 3D model more complexity and precision is added to the simulations. As problems with the COMSOL multiphysics solver (chapter 4.3) occurred, the 1D moisture diffusion model is used to present the results. The 3D model could be used to give more insight of the effect of stacked potatoes on the water loss. A further explanation of the choice for this 1D model can be found in chapter 4.3. The 1D model (Figure 3) can be more easily visualised as the red line in Figure 2.



Figure 3 schematic overview of the 1D moisture diffusion model

The model consist of temperature balances, mass balances for the water concentration and a momentum balance for the movement of the air.

The temperature balance for the air domain is:

$$d_z \rho_a C_{p_a} \frac{\partial T}{\partial t} + d_z \rho_a C_{p_a} u \nabla T - \nabla d_z k_a \nabla T = 0, \quad \text{in } (0, T_a] \times \Omega_a \quad (3-3)$$

For temperatures greater than 0, less or equal to the air temperature, T_a (K). With d_z as the thickness of the domain (m), ∇ the differential operator (m^{-1}), ρ_a the density of the air ($kg\ m^{-3}$), C_{p_a} the heat capacity of the air ($J\ kg^{-1}K^{-1}$), u the air speed ($m\ s^{-1}$) and k_a the thermal conductivity of air ($W\ m^{-1}K^{-1}$).

With the boundary conditions:

$$\frac{\partial T_a}{\partial x} = 0, \quad \text{on } [0, T_a] \times \partial\Omega_{a2} \quad (3-4)$$

$$T_p = T_a, \quad \text{on } [0, T_a] \times \partial\Omega_{a1} \quad (3-5)$$

And the initial condition:

$$T_a(0, j) = T_{a,0}, \quad \text{on } j \in \Omega_a \quad (3-6)$$

For the potato domain a similar temperature balance is used:

$$d_z \rho_p C_{p_p} \frac{\partial T}{\partial t} - \nabla d_z k_p \nabla T = 0, \quad \text{in } (0, T_a] \times \Omega_{p2} \quad (3-7)$$

Where the ρ_p the density of the potato ($kg\ m^{-3}$), C_{p_p} the heat capacity of the potato ($J\ kg^{-1}K^{-1}$), u the air speed ($m\ s^{-1}$), k_p the thermal conductivity of potato ($W\ m^{-1}K^{-1}$) and T_p the temperature of the potato (K).

With the boundary condition:

$$T_p = T_a, \quad \text{on } [0, T_a] \times \partial\Omega_{p_2} \quad (3-8)$$

$$\frac{\partial T_p}{\partial x} = 0, \quad \text{on } [0, T_p] \times \partial\Omega_{p_1} \quad (3-9)$$

And the initial condition:

$$T_p(0, j) = T_{p,0}, \quad \text{on } j \in \Omega_p \quad (3-10)$$

For the water concentration in the air the balance is:

$$\frac{\partial c_a}{\partial t} + u \nabla c_a - \nabla D_a \nabla^2 c_a = 0, \quad \text{in } (0, c_a] \times \Omega_a \quad (3-11)$$

With c_a the concentration water in the air (mol m^{-3}), D_a the diffusion coefficient of water in air (m s^{-2}).

With the following boundary conditions

$$c_a = c_{a_{in}}, \quad \text{on } [0, c_a] \times \partial\Omega_{a2} \quad (3-12)$$

Where $c_{a_{in}}$ is the concentration of water in the inflowing air.

$$kov(c_p - c_a) = D_a \nabla c_a - u c_a, \quad \text{on } [0, T_a] \times \partial\Omega_{a1} \quad (3-13)$$

Where c_p is the concentration water in the potato (mol m^{-3}) and kov the skin transfer coefficient (m s^{-1}).

And the following initial condition:

$$c_a(0, j) = c_{a,0}, \quad \text{on } j \in \Omega_a \quad (3-14)$$

The water concentration balance for the potato:

$$\frac{\partial c_p}{\partial t} - \nabla D_p \nabla^2 c_p = 0, \quad \text{in } (0, c_a] \times \Omega_p \quad (3-15)$$

Where D_p is the diffusion coefficient of water in potato (m s^{-2}).

With the boundary conditions:

$$kov(c_a - c_p) = D_p \nabla c_p, \quad \text{on } [0, T_a] \times \partial\Omega_{p_2} \quad (3-16)$$

$$\frac{\partial c_p}{\partial t} - \nabla D_p \nabla^2 c_p = 0, \quad \text{in } (0, c_a] \times \Omega_{p_1} \quad (3-17)$$

And the initial conditions:

$$c_p(0, j) = c_{p,0}, \quad \text{on } j \in \Omega_p \quad (3-18)$$

The flow is only in the air domain and only when the fan is on (FanState = on).

$$u = -0.267 \left[\frac{m}{s} \right] \text{ when } FanState = on, \quad u = 0 \left[\frac{m}{s} \right] \text{ when } FanState = off \text{ in } \Omega_a \quad (3-19)$$

With the boundary conditions:

$$\frac{\partial u}{\partial x} = 0, \quad \text{on } [0, c_a] \times \partial\Omega_{a1,2} \quad (3-20)$$

And initial conditions

$$u(0, j) = u_0, \quad \text{on } j \in \Omega_a \quad (3-21)$$

4 Simulating the skin moisture transfer coefficient

4.1 Materials

All calculations were performed on an Intel Xeon CPU E5-1650 with 3.20GHz, 3201 MHz, 6 Core(s) and 12 Logical Processor(s), containing 24 GB RAM and 25.9 GB Virtual memory. To perform a simulation with COMSOL Multiphysics 5.3 of a single week, for 14 parameter values (described in chapter 4.4), with 101 mesh points (the extremely fine mesh setting), took approximately 3.5 hours. Besides, Matlab 2015b was used for calculations and figures. The data used is measured in a commercial scale storage facility with sensors measuring every 5 minutes. The load cell used has an accuracy of 5 gram, the temperature sensors (pt100) of 0.1 °C and the used relative humidity sensor (HC101) an accuracy of 3%.

4.2 Parameters, variables and assumptions

The average dimensions of Miss Malina potatoes were determined (Table 1) out of the measurements of 1114 potatoes (Nik Grubben), the volume is calculated using the average length and width. Miss Malina potatoes have on average an ellipsoid/rod like shape in which the width is the diameter. The averages are used in the 3D moisture diffusion model (Table 1).

Table 1 rounded average characteristics of a MissMalina potato in storage

Length (L)	7.5 ± 1.8 cm
Width (W)	4.8 ± 0.9 cm
Volume (V_p)	9.05E-05 m ³
Weight per potato (W_p)	0.126 kg
Under water weight (UWW) Miss Malina	0.425 kg dry matter / 5 kg potato

The described length and width (Table 1) of the potato are used as parameters the 3D moisture diffusion model, the size of the air domain was chosen to be 7.5 by 5 cm. The reason and calculations can for the chosen air domain size can be found in Appendix D. The UWW was measured for potatoes from the same storage facility as the data, by Nik Grubben.

For the 1D moisture diffusion model the ellipsoid potato was deformed to get a square with the same length but a new width (Figure 4). This width ($1.2 * \pi$) was used. The air domain still had a width of 5 cm as changing this width does not have a notable effect (Appendix C). This results in Figure 3.

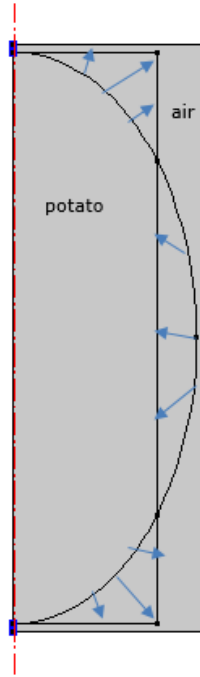


Figure 4 resizing the potato to find dimensions for 1D moisture diffusion model, the arrows indicate the way this was performed

COMSOL multiphysics contains a library with material properties like the thermal conductivity, density and heat capacity of the air. The potato and some air properties (Table 2) had to be added manually.

Table 2 manual added potato and air parameters

Moisture diffusion coefficient in air (D_a)	2.3E-05	m^2/s	Welty et al., 2009. The average air temperature (8.4°C) was used
Moisture diffusion coefficient in potato (D_p)	1.0E-09	m^2/s	Srikiatden & Roberts 2006 & 2008. Extrapolation of their results
Heat capacity potato (C_{p_p})	3430	$J/(kg\ K)$	Engineering Toolbox; Specific Heat of Food and Foodstuff
Thermal conductivity potato (k_p)	0.4	$W/(m\ K)$	Donsi, Ferrari & Nigro 1996
Density potato (ρ_p)	1391	kg/m^3	W_p/V_p
Thickens of the potato (d_z)	1	m	This is the standard setting. It doesn't make a difference if 1 m or the average potato size of 7.5 cm is used (Appendix D)

The sensor data of the commercial storage consisted of air temperature, potato temperature and relative humidity measured every 5 minutes and potato weight and a flow sensor measured at random moments. As the weight was taken of a bag of potatoes was use, the relative weight of the potato sample in the storage facility (rW_p) is used. The initial values for $T_a, T_p, RH, flow$ and rW_p where taken as the values on 22-11-2016 13:40:00, t=0 in the rest of this report.

Out of this sensor data, together with the above parameters the following variables where calculated (Table 3):

Table 3 variables used in both the 1D and 3D moisture diffusion model

Temperature incoming air (T_a)	$T_a(t)$	°C
Relative humidity incoming air (RH)	$RH(t)$	—
Initial water concentration in potato (c_{p0})	$\frac{W_p * (1 - UWW) * rW_p(t)}{V_p * MW_w}, \text{ with } t = 0$	mol/m^3
Water concentration in air (c_{a0})	$\frac{RH(t) - (RH_{max} - 100)}{100} * \frac{\rho_{sat}(T_a(t))}{R * T_a(t)}, \text{ with } t = 0$	mol/m^3
Water concentration incoming air ($c_{a,in}$)	$\frac{RH(t) - (RH_{max} - 100)}{100} * \frac{\rho_{sat}(T_a(t))}{R * T_a(t)}$	mol/m^3

All assumptions:

- The potato is a perfect ellipsoid within the 3D model
- No sprouting occurred during storage
- Lenticels are not taken into account
- Good quality potatoes (no skin cuts, no pressure bruising, no rotting) were used
- All water can be extracted from the potato
- The potato has a homogenous water concentration at the start
- Storage conditions are homogenous at the start
- No condensation of water happens when the relative humidity becomes bigger than 100% A manual stop of the water transport through the skin was implemented.

4.3 Model evaluations

To visualise some phenomena the 3D moisture diffusion simulations are used till 6 days of simulation. For the determine if the membrane diffusion model could be used a simulation was performed with the 3D moisture diffusion model, since the 3D model gives the clearest indication of how the water is distributed within the potato. This simulation contained all data from the storage facility and should run from $t=0$ to $t=79.4$ days with the current state of the system saved every 5 minutes. 79.4 days was the last moment for which data was available. The solver was not allowed to take bigger steps than 4-minute steps, this to ensure no events like fan on or fan going off would be ignored by the solver. This simulation encountered singularities after 6.2 days. This happens due to too fast big changes within the simulation, probably close to the boundaries of the system (personal communication Sander Bezuijen (COMSOL)). In Figure 5 the distribution of the water around the potato can be seen.

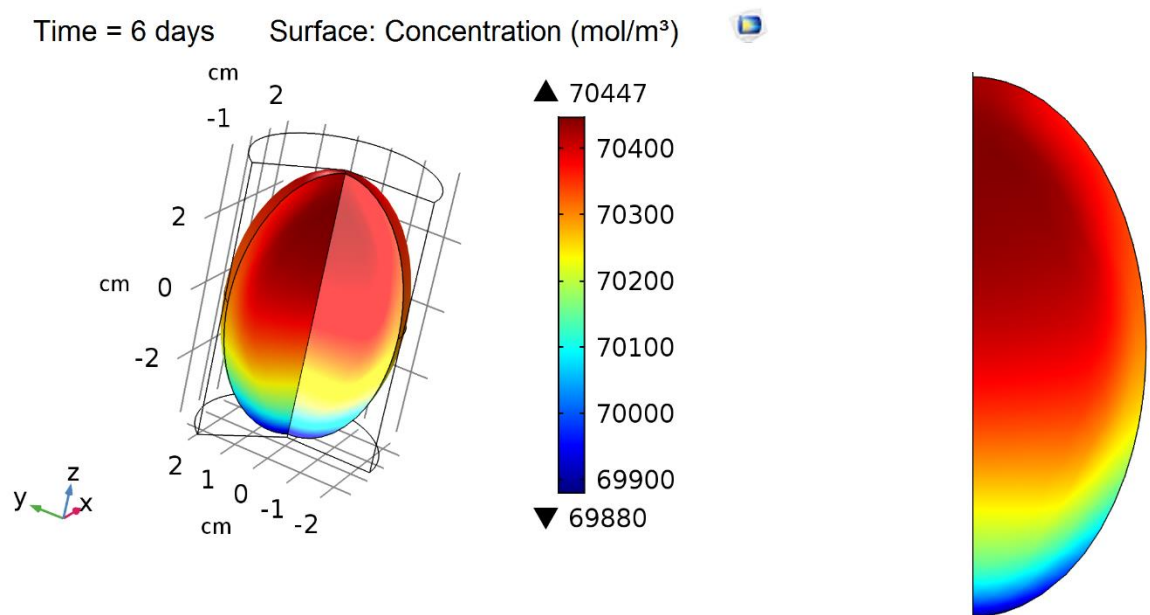


Figure 5 3D and 2D image of the water distribution within the potato after 6 days, legend holds for both images

As can be seen in Figure 5 the concentrations are in the same order of magnitude distributed over the potato, the concentrations are not homogenous. Although the order of magnitude of the water concentration in the center and near the skin is the same, the membrane diffusion model would only be able to calculate the development of the skin transfer coefficient afterwards. Therefore, the membrane diffusion model is not used. Besides, the airflow is not taken into account in the membrane diffusion model, although this is one of the variables which can be regulated by the owner of the storage. As the 1D CFD and 3D CFD moisture diffusion models made within COMSOL multiphysics are able to predict the moisture diffusion coefficient of the skin (k_{ov}) depending on the regulated airflow, temperature and relative humidity, these models will be used.

The weight loss of the potatoes in storage was measured and becomes smaller over time (Figure 6). Based on this knowledge the skin moisture transfer coefficient is expected to decrease. As the driving force, the difference between the water concentration in the potato and in the air (equation (3-1)), is expected to be continuous in the same order of magnitude.

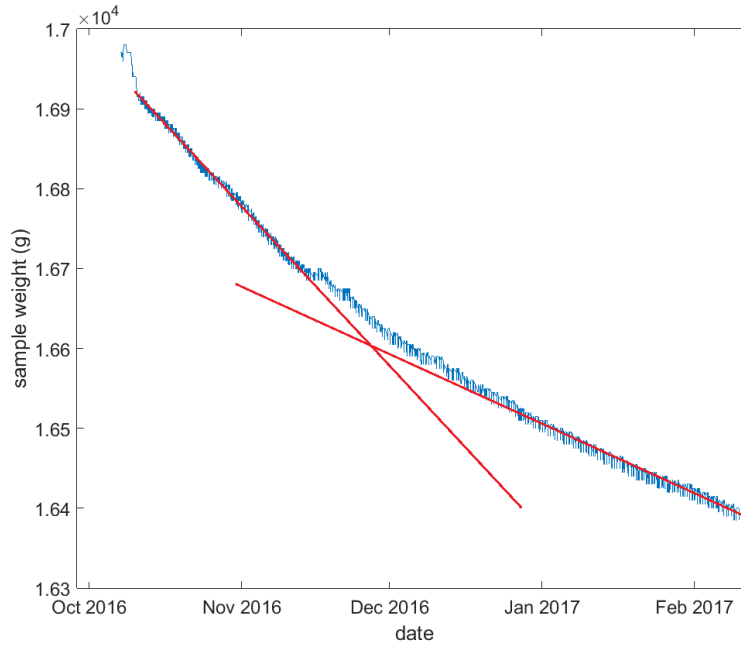


Figure 6 the measured weight loss over storage time, measured using a scale in a commercial storage facility. Red lines are manual added tangent lines to show an approximate of the slope of the start and final data points.

4.4 Model calibration

The model calibration was performed using the 1D moisture diffusion model. The sensor data was used and simulations of 7 days were performed, to find the best skin moisture transfer coefficient. The skin moisture transfer coefficient (k_{ov}) was varied with discrete steps between $1E-10$ till $1E-08$ in a logarithmic way with 5 steps per decade. In total 12 parameter values were tested. When $1E-08$ was not sufficient anymore the range was extended in the same way to $1E-07$, this results in the steps presented in Figure 7.

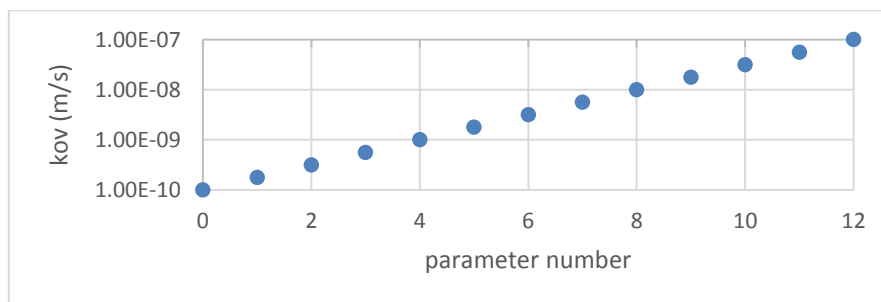


Figure 7 all used parameter values for k_{ov} (m/s)

Every 5 minutes the water concentration was noted by COMSOL. With the use of Matlab the sum of squared errors (SSE) of the measured data in comparison with the simulation result was calculated. To be able to use the measured data it was interpolated and the same time steps as the simulation results were taken. The best fitting k_{ov} values are shown in Figure 8, the calculated SSE for all tested k_{ov} values can be found in Appendix G. When the second best k_{ov} value, regarding the SSE, was used, this was due to a weight factor, visually examined, placed on the end point. As can be seen in Figure 8 the k_{ov} tends to increase over time.

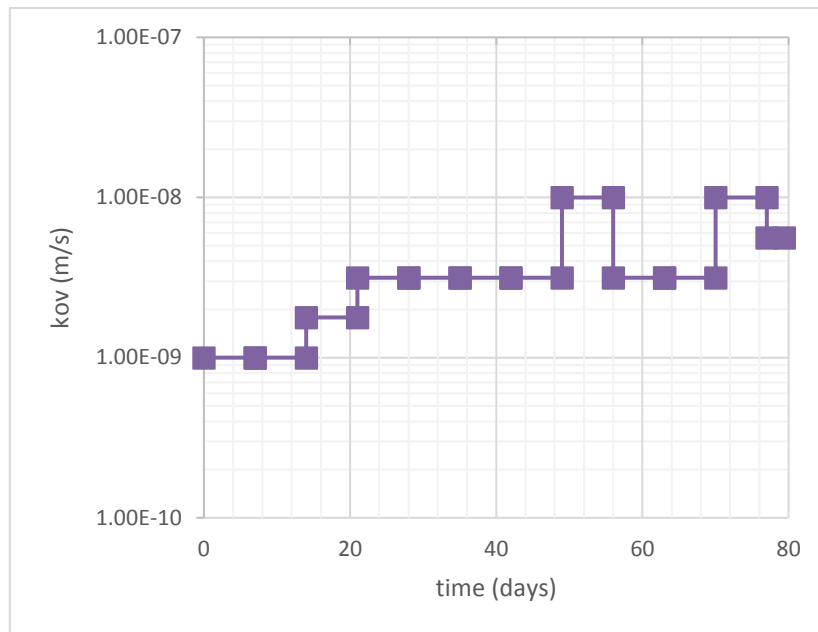


Figure 8 kov over time

This curve (Figure 8) was loaded as input value and the model was run from $t=0$ till $t=79.4$ days and compared with the measured data.

The results of this first calibration can be seen in Figure 9, the simulated result did not resemble the data at all. This was not expected looking at the results for the simulations in steps per week (Figure 10).

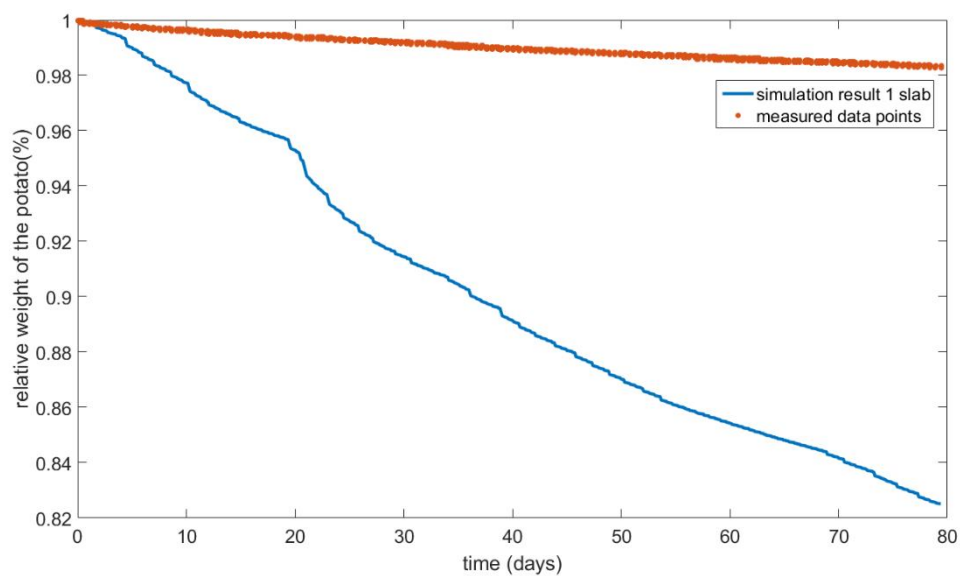


Figure 9 relative weight percentage of the potato over time. The red dots are the measured data values, the blue line the simulated relative weight when performing a full period simulation with the best fitting kov values for each week.

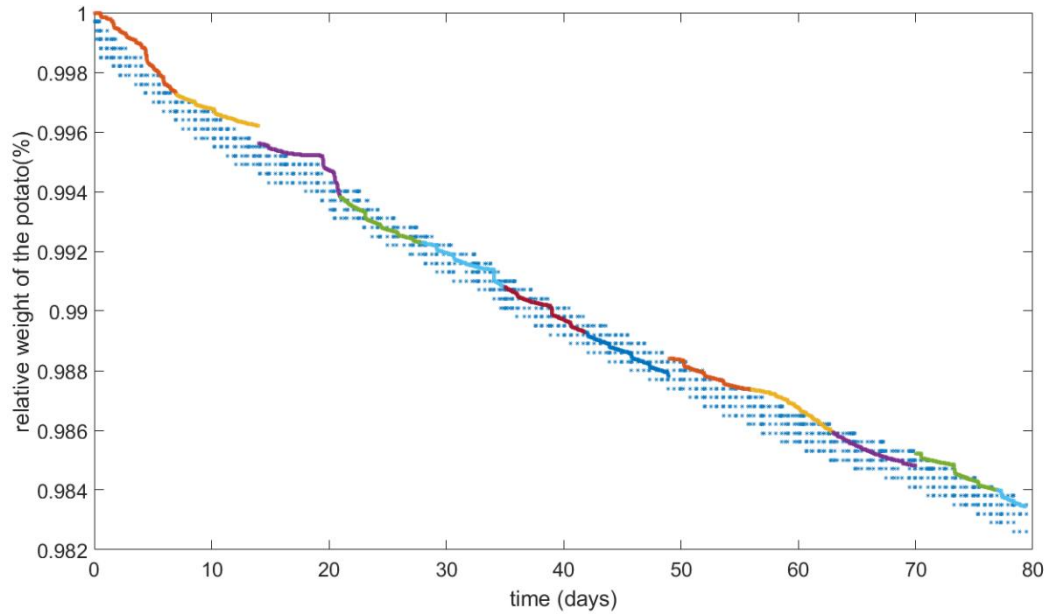


Figure 10 relative weight percentage of the potato over time. The blue dots are the measured data points, the coloured lines are the relative weights of the potato for the best fitting calibration simulated per week.

Probably the reason for the difference between Figure 9 and Figure 10 is the simulation of only a week at a time instead of the full storage time. When a new weak is started the start concentration of water in the potato is recalculated and homogenous for the potato.

To check the hypothesis of the homogenous start every week, a new experiment was performed in which the potato was divided into two, four and 12 parts/slabs in the way described in Table 4. To this different experiments will be referred as the 2, 4 or 12 slab simulations.

Table 4 slab sizes for the different simulations

Number of slabs	Boundaries of the slabs
2	$0 - 0.6\pi$, $0.6\pi - 1.2\pi$
4	$0 - 0.5\pi$, $0.5\pi - 0.8\pi$, $0.8\pi - 1.1\pi$, $1.1\pi - 1.2\pi$
12	$0 - 0.1\pi$, $0.1\pi - 0.2\pi$, $0.2\pi - 0.3\pi$, $0.3\pi - 0.4\pi$, $0.4\pi - 0.5\pi$, $0.5\pi - 0.6\pi$, $0.6\pi - 0.7\pi$, $0.7\pi - 0.8\pi$, $0.8\pi - 0.9\pi$, $0.9\pi - 1.0\pi$, $1.0\pi - 1.1\pi$, $1.1\pi - 1.2\pi$

At first the 2 slabs was tested, in this simulations the average concentration of the slab was used as a new initial concentration for the next simulation week, to lower the effect of the weekly homogenisation of the water concentration of the potato. Due to the results of 2 slabs, the 4 and 12 slabs division of the potato was tested. The size of these 4 slabs was chosen due the expected spreading of the water in the potato (Figure 5), as near the skin more differences in water concentration are found than near the core. The COMSOL multiphysics software is, to the best of my knowledge, unable, to continue with all the last concentration values of the parameter sweep as initial

values for the next simulation. An approximation was performed with 12 slabs, since using smaller domains would be very time consuming.

The best fitting k_{ov} values are shown in Figure 11, the calculated SSE for all tested k_{ov} values can be found in Appendix G. As can be seen in Figure 11 no big differences in the best k_{ov} values for the different simulations are present. However, when looking at Figure 12, where a full simulation over time with the best k_{ov} was performed, quite some differences between the potato as a whole and the potato divided into slabs was noted.

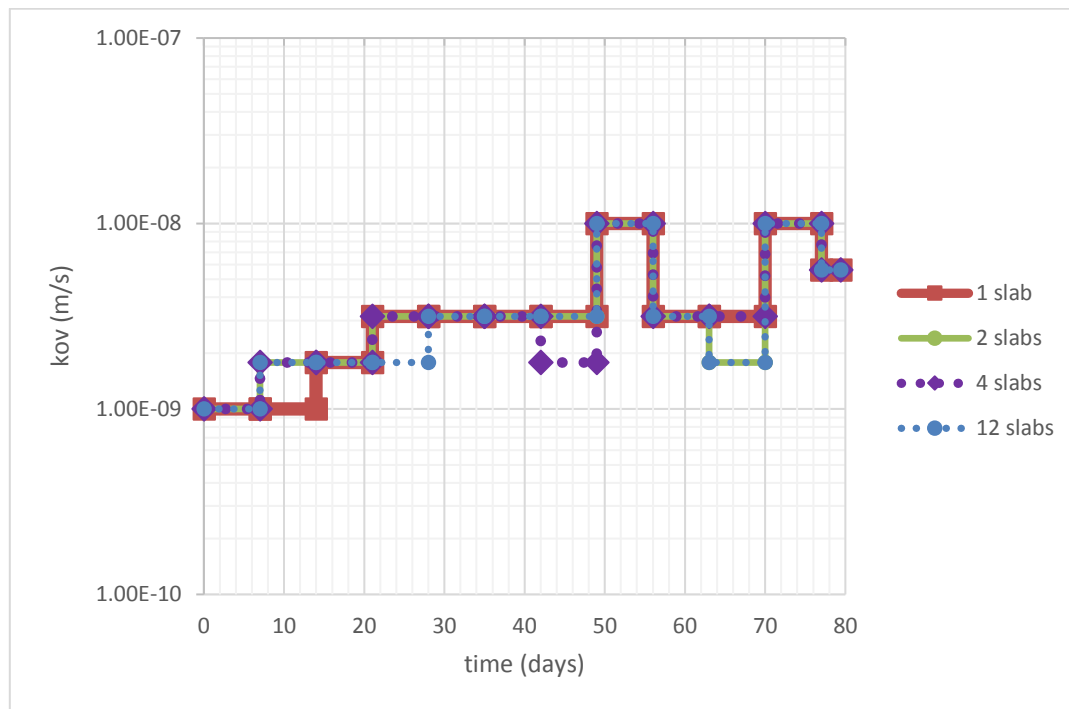


Figure 11 the best k_{ov} over time for the different simulation types: red for the potato as whole, green for the potato divided in 2 slabs, purple for the potato divided in 4 slabs and blue for the potato in 12 slabs.

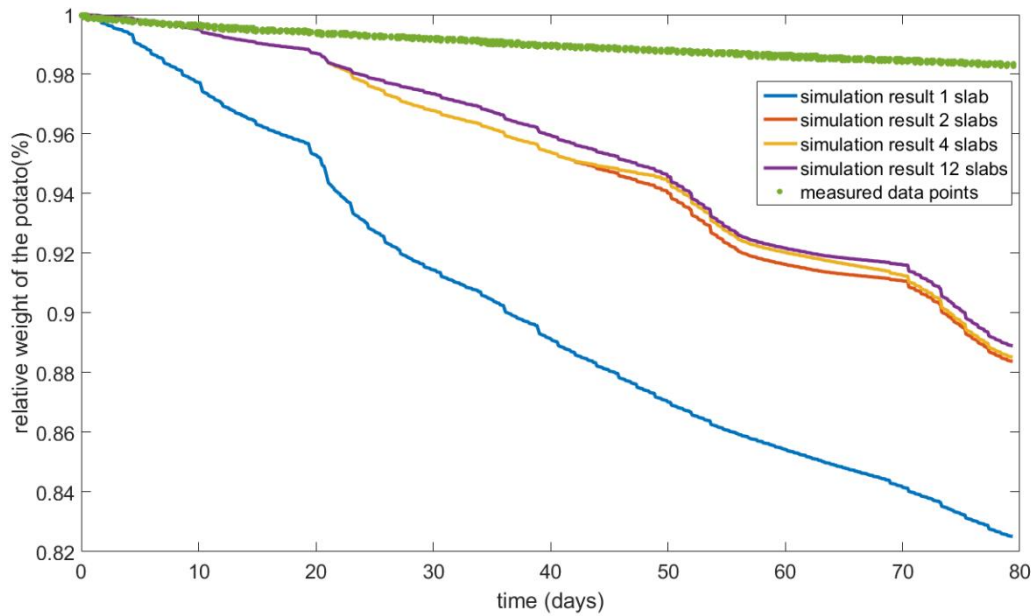


Figure 12 relative weight percentage of the potato over time. The green dots are the measured data values, the blue line the simulated relative weight for a potato division in 1 slab, red for 2 slab division, yellow for a 4 slab division and purple for a 12 slab division.

As can be seen in Figure 12, the 2 slab simulation has a better fit than when the potato is simulated as a whole (1 slab). Further increasing the number of slabs did not increase the fitted value that much. Therefore, this is not the full solution to a working model.

The most peculiar result is Figure 10 in this figure the relative weight of the separate weeks is shown and fits on the measured data, 2, 4 & 12 slabs showed the same behaviour (results not shown). Of course this was expected, as the kov of the best fitting result was taken. These results were taken to create the kov curves (Figure 11), however when running all weeks at once the result is completely off (Figure 12). To perform full period calibration experiments the model used to create the kov curve was only changed at 3 points. All 3 changes between the models were evaluated. First, instead of simulating for 7 days, simulations were performed for 79.4 days. Checking if the solver shows strange behaviour due to this change is not possible, the solver is reinitialized every time the fan goes on, and in my personal opinion highly unlikely. Secondly, the initial values did not have to be set every week but only at the start of the simulation. Therefore, the slabs were not homogenised after each 7 days. The steps explained above resulting in Figure 12 ensure the problem is not solely in this change between the models. Finally, the parameter sweep was turned off and the kov values were loaded as a function. In Figure 13 the used kov values within COMSOL are shown for the 4 slabs simulations, these curves are the same as Figure 11. Thus, COMSOL does not make an error within this translation step.

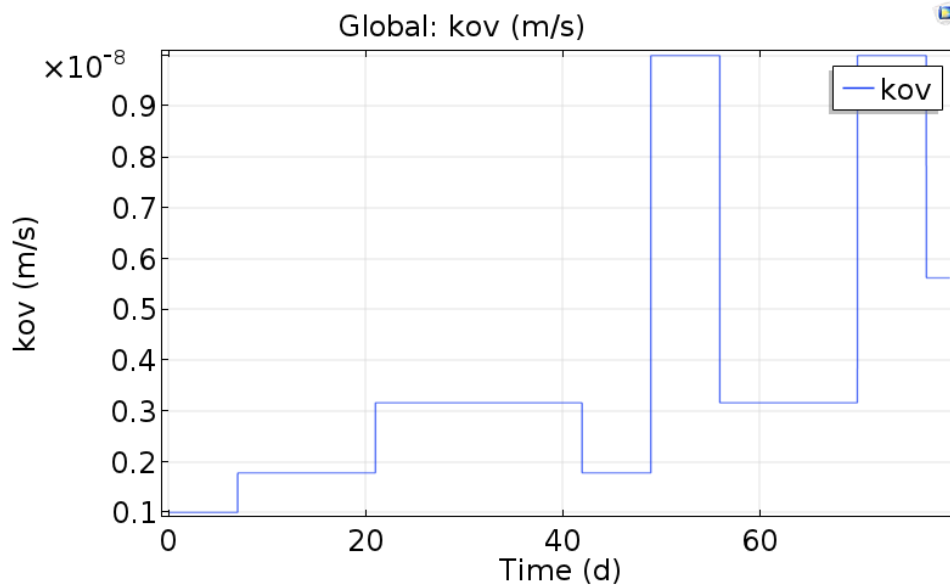


Figure 13 kov over time used within the 4 slab simulation

As the full storage period simulations did not fit on the measured data, a new hypothesis was formed. Due to the discretised parameter values, abrupt changes within the kov value happen. For example, in Figure 12, the first weeks of the 2, 4 and 12 slab simulations show a good fit until somewhere in week 4, at week 5 a new kov value is applied. The COMSOL solver can get off due to fast and abrupt changes. To check the hypothesis, which states that these abrupt changes let the solver behave in an unexpected way, a new simulation was performed with the 12 slabs model for week 5, 6 and 7, as these 3 weeks have a constant kov value. For the initial water concentration, the start concentration times the relative weight percentage of the measured data was used. As can be seen in Figure 14 the simulation fits well on the measured data points. This means the model is working fine when the initial values for the water concentration in the potato are correct and no changes occur with the kov value, which is consistent with the findings represented in Figure 10.

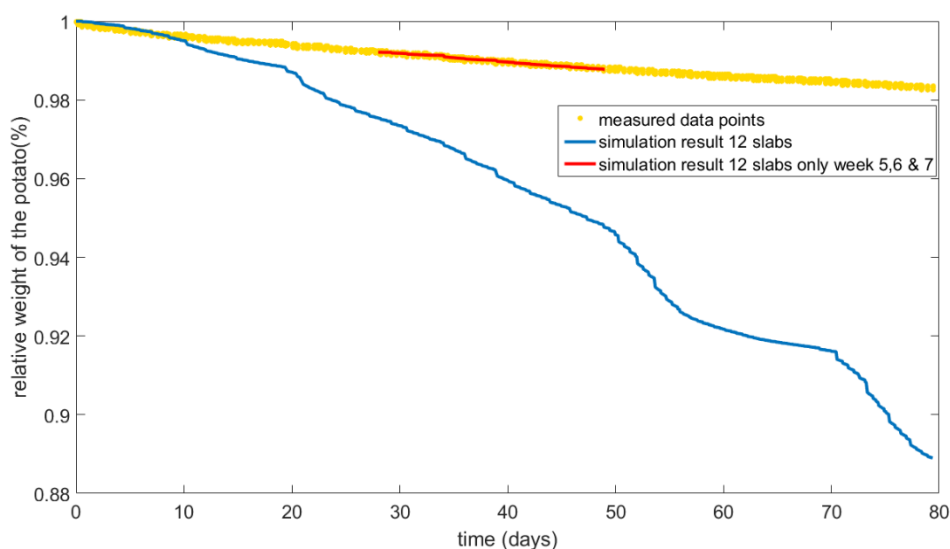


Figure 14 relative weight percentage of the potato over time. The yellow dots are the measured data values, the blue line the simulated relative weight for a potato division in 12 slabs. The red line is a

simulation with 12 slabs over week 5, 6 and 7 using as initial weight loss the measured data point at the start of week 5.

Therefore, although the simulation over the full storage period does not fit that well, the weekly simulations do (Figure 10). This means that the model can be used and the determined kov values in Figure 11 are correct. To prove that the kov is changing over time, like Figure 11 shows, a simulation with the average kov of the 12 slabs simulations, $3.76\text{E-}09\text{ m/s}$, was performed. As can be seen in Figure 15, the average kov has a worse fit in comparison with the one where the kov increased over time. Therefore, kov is changing over time. Next to this, a simulation was performed with a constant kov of $1\text{E-}11\text{ m/s}$ and $1\text{E-}10\text{ m/s}$, as can be seen there is almost no weight loss present with this kov values.

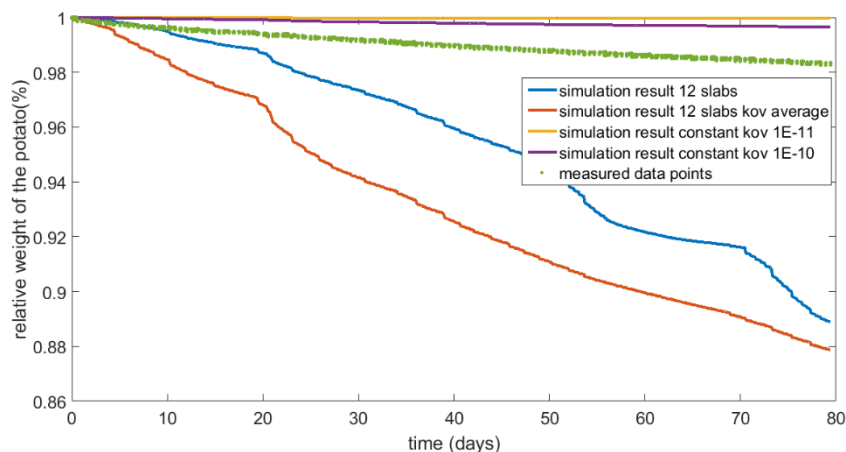


Figure 15 relative weight percentage of the potato over time. The green dots are the measured data values, the blue line the simulated relative weight for a potato division in 12 slabs. The red line is a simulation with the average kov for the 12 slabs. The yellow line is the relative weight for a potato with a constant kov of $1\text{E-}11\text{ m/s}$ and the purple line the relative weight for a potato with a constant kov of $1\text{E-}10\text{ m/s}$.

5 Discussion & recommendations

Within pears the skin moisture diffusion rate was determined to be around $5\text{E-}09$ m/s (Nguyen et al, 2006a). For apples the skin moisture diffusion rate was determined for 3 varieties of apples, all ranged between $5\text{E-}10$ m/s and $4\text{E-}9$ m/s (Veraverbeke et al., 2003). However, all not measured over time. Looking at the order of magnitude it can be concluded that potatoes loss water more rapid than the other commodities.

Lendzian (2006) found opposite results, in comparison with the results found during this thesis. Lendzian' results are coming from laboratory experiments with enzymatically isolated cuticles of potatoes. The permeance ($m\ s^{-1}$), defined as $\frac{\text{rate of water loss } F\ (g\ s^{-1})}{\text{pneum area } A\ (m^2) * \text{driving force } \Delta c\ (g\ m^{-3})}$, of 3 different potato varieties decreased with a factor 3.3-25 during the first few days and became stable after 2 weeks of storage, in total the potatoes were in storage for 9 months. Within this thesis an increase was observed. Lendzian could not explain the decrease of permeance according to the chemical changes (suberin polymer, soluble lipids and waxes) of the periderm, as the permeance did not change while the suberin increased and lipids decreased. Maybe this is due to the enzymatic isolation, other molecules or connections can be broken and influence the results. Although Lendzian did not found a correlation between permeance and chemical changes, it can be present. Thus, it would be wise to analyse the chemical composition of the skin over time, while also performing the measurements gathering the data for the model.

Moreover, all mentioned processes in chapter 2.2, could have happened within the storage facility. As the quality was not mentioned within the data it was assumed that the quality of the potatoes both at the start as in the end was good. The processes and quality factors, like the degradation of starch (Biemelt et al., 2000), respiration, mould, pressure bruised potatoes and skin damaged potatoes, are not taken into account in this model, however influencing the weight of the potatoes and therefore combined in the k_{ov} , since the k_{ov} is based on the measured weight.

Due to the simulation with a constant k_{ov} value of $1\text{E-}11$ m/s, Figure 15, it can be concluded that the model does have an error, as with a much larger constant k_{ov} a better fit is gained in comparison with the changing k_{ov} . However, with this lower k_{ov} value the water loss was underestimated. With a k_{ov} value of $1\text{E-}10$ m/s a better fit was obtained, still underestimated. The average k_{ov} for the 12 slab simulation ($3.76\text{E-}09$ m/s) performed much worse and was an overestimation of the water loss. While, this k_{ov} value is only a factor 2.65 larger. Such a big difference in result suggest that the model is really sensitive to k_{ov} or the model is wrong.

The changing k_{ov} was fitted every week (Figure 10) and normally should not deviate significant from the simulation with all of these values combined. The weekly fitting resulted in 12 times fitting, this includes 12 times a small model error within the fitted parameter, in the end this gave a big offset. This is one of the risks using a full white box model with only 1 parameter, as this gives a very inflexible model the parameter value is forced towards the data in the best possible way, independent of the model. As there was only 1 data set some errors could be made, like excluding relevant system inputs, like the CO_2 level or another process, also unmeasurable variation can be easily included within the parameter estimates and due to only 1 data set not reduced. Due to the sensitivity of the model towards k_{ov} , the increasing error using bigger time steps and the discretised parameter values no good fit was obtained. During the conclusion the result of the weekly time step model is used.

To determine the total water concentration the UWW (underwater weight) is used, this is a specific number per harvest per variety. This UWW shows the total amount of non-water within the potato, the complementary part (1-UWW) is the total amount of water within the potato. This is both bound water and free water. Only 13% of the total amount is free water, 81% is loosely bound water (Khan et al., 2016). As no models for the release of loosely bound water are present, the choice was made to calculate with all water. Since the relative weight is used, the effect of this choice is lowered, however still present. With less water within the potato, when the water loss stays the same, the driving force becomes lower resulting in a bigger k_{ov} .

Furthermore, it is unknown whether the change of resistance of the skin to water loss is due to a change in the composition of the periderm and/or outer cortex. The size of these layers can change over time or even a new layer can be formed. And in both cases, the chemical composition of the skin can change. When the composition changes, the diffusion coefficient will also change. For example, in the more studied apples a wax layer will cover cracks in the peel to protect for moisture loss (Veraverbeke et al., 2001). Still structure loss of the apples was observed after an eight-month storage period. This wax layer increases the thickness of the skin and changes the composition which both influence the diffusion coefficient of the skin. Unfortunately, it is not possible to determine these phenomena using the available data. To include both possible processes the mass transfer coefficient was modelled, this is the diffusion coefficient divided by the thickness of the skin: $\left(k_{ov} = \frac{D_{skin}}{d_{skin}}\right)$ (equation (3-2)).

A method to measure the thickness of different tissues in apple (wax, cutin and cuticle) is known (Veraverbeke et al., 2001), which could be applied to potatoes. This method uses a gold coating and microscopy techniques. Which is a costly and challenging, but a non-destructive way of measuring. A destructive way of measuring the diffusion coefficient of the same different tissue samples exists (Veraverbeke et al., 2003). Here the weight loss of the sample is measured over time. A mannitol solution should be used as diffusing agent in order to approximate the water activity of apple juice. As apples and potatoes are commodities, it is not needed to be very thrifty with them, therefore the destructive way of measuring can be performed. When the change of the thickness of the skin is known it can be investigated where the change in skin permeability is coming from; the increasing thickness, the change in composition or both.

A physical and time limitation of this research is that potatoes are harvested only once a year. Meaning that the storage experiments can only be started in a short time period, because the data should contain the full storage period. Only data of previous storages periods was used in this model, since this thesis was started after the harvest season, so, no experiments could have been performed to test parameters like airspeed, ventilation time. Moreover, the data used is coming from one single setup, no triplicate measurements were used. In a study where the barrier properties of the skin improved, relative humidity and temperature did not influence this improvement (Schreiber et al., 2005). In the data set used is a big lack of data, as sensors did not respond for a month and the potatoes were sold very early in the season. When having more data, the observed trend of a decrease in water loss (Figure 6) could be investigated more. Does it decrease further or even become zero or does it become linear, which looking at Figure 6, is currently the case. A linear decrease means a further increasing k_{ov} , as the driving force becomes lower and the weight loss is constant (equation (3-1)(3-2)).

First, the model should be calibrated well. An in-depth analysis of the possible errors within the COMSOL extraction of the k_{ov} values should be made. When the model is calibrated well, it can be extended with more processes happening within the potato, to get more insights in the effect of a certain process and the storage climate regarding the water loss of the potato. An extensive model is present for the distribution of water within a pear during post-harvest storage (Nguyen et al., 2006b). To implement this model for potatoes more data should be gathered. Knowing how the water is distributed within the potato can give new insights in strategies to prevent bruising or other types of appearance and quality loss. Moreover, it can give a good insight in where along the potato skin the resistance to water loss is higher. Resulting in different storage strategies in order to decrease the overall water loss.

Furthermore, the cortex tissue of a pear consists of cells and intercellular spaces of various different shapes and sizes (Verboven et al., 2008). The transport of water is, modelled using various diffusion laws and thermodynamics (Noble 1991). Full derivations of the diffusion equations for these cell structures are present (Fanta et al., 2013 & 2014). These equations even take cell shrinkage into account. However, a lot more precise experiments have to be performed to find all parameter values for potatoes.

However, increasing the precision of the model will increase the computational time. A trade-off has to be found between the level of complexity of the model and the computational costs. Consequently, sensitivity analyses should be performed to find the important processes within the potato. The results of these analyses will give insight on which parts of the model more detail should be added. However, the level of detail should correspond with the objective of the model.

6 Conclusion

During long time potato storage, the potatoes loss quality and water, which has a major impact on the income of farmers, as it influences the two factors determining the potato price: the quality and the weight of the potatoes. Water loss, mainly caused by evaporation and respiration can result in bruising, discoloration, peeling losses, and worse culinary quality. Other types of quality loss like moulds and pressure bruising are strengthened by water loss. The process of water loss is influenced by the skin characteristics, like thickness, the presence of lenticels and wounds.

The skin thickness and the moisture diffusion coefficient of the skin, both influencing the rate of moisture loss through the skin, are modelled within a 1D moisture diffusion model. This model was calibrated on the skin moisture transfer coefficient, which is the ratio of the moisture diffusion coefficient of the skin over the skin thickness. Out of the simulations comparing a changing skin moisture transfer coefficient with a constant skin moisture transfer coefficient (Figure 15) there can be concluded that the skin moisture transfer coefficient is changing over time. According to Figure 11, increasing over time.

The increase of the skin moisture transfer coefficient over time, means an increase in the ratio of the diffusion coefficient over the skin thickness. As the skin thickness is believed to increase during storage, the diffusion coefficient becomes larger. Since the skin moisture transfer coefficient increases over time, the current used storage regime is not suitable to minimize water loss. Using this model, optimization of the storage conditions can be performed.

7 References

- Adams, M. J. (1975). Potato tuber lenticels: development and structure. *Annals of applied biology*, 79(3), 265-273.
- Adams, M. J., & Griffith, R. L. (1978). The effect of harvest date and duration of wound healing conditions on the susceptibility of damaged potato tubers to infection by *Phoma exigua* (gangrene). *Annals of applied Biology*, 88(1), 51-55.
- Allen, J. D. (1957). The development of potato skin-spot disease. *Annals of Applied Biology*, 45(2), 293-298.
- Bentini, M., Caprara, C., & Martelli, R. (2006). Harvesting damage to potato tubers by analysis of impacts recorded with an instrumented sphere. *Biosystems Engineering*, 94(1), 75-85.
- Bernards, M. A. (2002). Demystifying suberin. *Canadian Journal of Botany*, 80(3), 227-240.
- Biemelt, S., Hajirezaei, M., Hentschel, E., & Sonnewald, U. (2000). Comparative analysis of abscisic acid content and starch degradation during storage of tubers harvested from different potato varieties. *Potato Research*, 43(4), 371-382.
- Bird, R. B., Stewart, W. E., & Lightfoot, E. N. (2007). *Transport phenomena*. John Wiley & Sons.
- Blenkinsop, R. W., Copp, L. J., Yada, R. Y., & Marangoni, A. G. (2002). Changes in compositional parameters of tubers of potato (*Solanum tuberosum*) during low-temperature storage and their relationship to chip processing quality. *Journal of Agricultural and Food Chemistry*, 50(16), 4545-4553.
- Bojanowski, A., Avis, T. J., Pelletier, S., & Tweddell, R. J. (2013). Management of potato dry rot. *Postharvest Biology and Technology*, 84, 99-109. Chicago
- Buck Research Manual (1996); updated equation from Buck, A. L., New equations for computing vapor pressure and enhancement factor, *J. Appl. Meteorol.*, 20, 1527-1532, 1981
- Butcbaker, A. F., Promersberger, W. J., & Nelson, D. C. (1973). *Respiration and Weight Losses of Potatoes during Storage*.
- Chourasia, M. K., & Goswami, T. K. (2006a). Simulation of transport phenomena during natural convection cooling of bagged potatoes in cold storage, Part I: Fluid flow and heat transfer. *Biosystems engineering*, 94(1), 33-45.
- Chourasia, M. K., & Goswami, T. K. (2006b). Simulation of transport phenomena during natural convection cooling of bagged potatoes in cold storage, Part II: Mass transfer. *Biosystems engineering*, 94(2), 207-219.
- Chourasia, M. K., & Goswami, T. K. (2006c). Model to predict the cool-down characteristics of variable air temperature potato cold storage using computational fluid dynamics. *Journal of food process engineering*, 29(6), 633-650.

- Chourasia, M. K., & Goswami, T. K. (2007a). CFD simulation of effects of operating parameters and product on heat transfer and moisture loss in the stack of bagged potatoes. *Journal of Food Engineering*, 80(3), 947-960.
- Chourasia, M. K., & Goswami, T. K. (2007b). Simulation of effect of stack dimensions and stacking arrangement on cool-down characteristics of potato in a cold store by computational fluid dynamics. *Biosystems Engineering*, 96(4), 503-515.
- Chourasia, M. K., & Goswami, T. K. (2007c). Steady state CFD modelling of airflow, heat transfer and moisture loss in a commercial potato cold store. *International Journal of Refrigeration*, 30(4), 672-689.
- Chourasia, M. K., & Goswami, T. K. (2007d). Three dimensional modelling on airflow, heat and mass transfer in partially impermeable enclosure containing agricultural produce during natural convective cooling. *Energy conversion and management*, 48(7), 2136-2149.
- Chourasia, M. K., & Goswami, T. K. (2008). Product-cooling load and moisture loss under different loading patterns and cooling rates of potatoes in cold storage. *Journal of food process engineering*, 31(3), 339-353.
- Chourasia, M. K., Goswami, T. K., & Chowdhury, K. (1999). Temperature profiles during cold storage of bagged potatoes: Effects of geometric and operating parameters. *Transactions of the ASAE*, 42(5), 1345-1351.
- Chourasia, M. K., Maji, P., Baskey, A., & Goswami, T. K. (2005). Estimation of moisture loss from the cooling data of potatoes. *Journal of Food Process Engineering*, 28(4), 397-416.
- Chourasia, M. K., Maji, P., Goswami, T. K., & Baskey, A. (2006). Cool-down characteristics of potatoes in commercial cold store. *Journal of food science and technology-mysore*, 43(4), 366-369.
- Chourasia, M. K., Sara, R., De, A., & Sahoo, P. Y. (2004). Evaluation of storage losses in a commercial potato cold storage. *JOURNAL OF FOOD SCIENCE AND TECHNOLOGY-MYSORE*, 41(5), 507-510.
- COMSOL Multiphysics® v. 5.3. www.comsol.com. COMSOL AB, Stockholm, Sweden.
- CTGB Toelating databank, College voor de toelating van gewasbeschermingsmiddelen en biociden. Accessed on 24-11-2016
- Daniels-Lake, B., Prange, R., Walsh, J., Hiltz, K., Bishop, S., & Munro-Pennell, K. (2014). Effects of simulated harvest injury and relative humidity during the first week post-harvest on potato (*Solanum tuberosum* L.) tuber weight loss during subsequent storage. *The Journal of Horticultural Science and Biotechnology*, 89(2), 167-172.
- Donsi, G., Ferrari, G., & Nigro, R. (1996). Experimental determination of thermal conductivity of apple and potato at different moisture contents. *Journal of food engineering*, 30(3-4), 263-268.
- Driskill, E. P., Knowles, L. O., & Knowles, N. R. (2007). Temperature-induced changes in potato processing quality during storage are modulated by tuber maturity. *American Journal of potato research*, 84(5), 367-383.

Effmert, B., Meinl, G., & Vogel, J. (1961). Atmung, Zuckerspiegel und Ascorbinsäure-Gehalt von Kartoffelsorten bei verschiedenen Lagertemperaturen. *TAG Theoretical and Applied Genetics*, 31(1), 23-32.

Engineering Toolbox; Specific Heat of Food and Foodstuff

https://www.engineeringtoolbox.com/specific-heat-capacity-food-d_295.html

last visited on 15-11-2017 10:00h

Fanta, S. W., Abera, M. K., Aregawi, W. A., Ho, Q. T., Verboven, P., Carmeliet, J., & Nicolai, B. M. (2014). Microscale modeling of coupled water transport and mechanical deformation of fruit tissue during dehydration. *Journal of Food Engineering*, 124, 86-96.

Fanta, S. W., Abera, M. K., Ho, Q. T., Verboven, P., Carmeliet, J., & Nicolai, B. M. (2013). Microscale modeling of water transport in fruit tissue. *Journal of Food Engineering*, 118(2), 229-237.

FAO (2014). FAOSTAT database collections. Food and Agriculture Organization of the United Nations. Rome. Access date: 2016-11-17.

Firman, D. M., & Allen, E. J. (2007). Agronomic practices. *Potato Biology and Biotechnology, Advances and Perspectives*, edited by D. Vreudgenhil, J. Bradshaw, C. Gebhardt, F. Govers, DKL MacKerron et al. Elsevier, Amsterdam, 719-738.

Groh, B., Hübner, C., & Lenzian, K. J. (2002). Water and oxygen permeance of phellem isolated from trees: the role of waxes and lenticels. *Planta*, 215(5), 794-801.

Grubben, N. L., & Keesman, K. J. (2015). Modelling ventilated bulk storage of agromaterials: A review. *Computers and Electronics in Agriculture*, 114, 285-295.

Hardenburg, E. V. (1949). Effect of types of container, storage and variety on shrinkage of stored potatoes. *American Potato Journal*, 26(3), 75-79.

Haverkort, A. J., & Struik, P. C. (Eds.). (2005). *Potato in Progress: Science Meets Practice*. Wageningen Academic Pub.

Heltoft, P., Wold, A. B., & Molteberg, E. L. (2016). Effect of ventilation strategy on storage quality indicators of processing potatoes with different maturity levels at harvest. *Postharvest Biology and Technology*, 117, 21-29.

Hooker, W. J. (1981). *Compendium of potato diseases* (Vol. 8). International Potato Center.

Janssen, A. E. (2014). Lecture slides chapter 7, course FPE-31306 november & december 2014

Khan, M. I. H., Wellard, R. M., Nagy, S. A., Joardder, M. U. H., & Karim, M. A. (2016). Investigation of bound and free water in plant-based food material using NMR T 2 relaxometry. *Innovative Food Science & Emerging Technologies*, 38, 252-261.

Kilpatrick, P. W., Lowe, E., & Van Arsdel, W. B. (1955). Tunnel dehydrators for fruits and vegetables. *Advances in food research*, 6, 313-372.

- Kleinschmidt, G., & Thornton, M. (1991). Bruise-free potatoes: our goal. Bulletin-Idaho Agricultural Experiment Station (USA). No. 725.
- Lendzian, K. J. (2006). Survival strategies of plants during secondary growth: barrier properties of phellements and lenticels towards water, oxygen, and carbon dioxide. *Journal of Experimental Botany*, 57(11), 2535-2546.
- Loon, C.D. van, A. Veerman, C.B. Bus & S. Zwanepol (1993). Teelt van consumptieaardappelen. Teelthandleiding 57, PAGV, Lelystad, 142 pp.
- Loon, K. D. van (2007). The seed potato market. *Potato biology and biotechnology: advances and perspectives*, 45.
- Lulai, E. C., Glynn, M. T., & Orr, P. H. (1996). Cellular changes and physiological responses to tuber pressure-bruising. *American Journal of Potato Research*, 73(5), 197-209.
- Lulai, E. C. (2007). Skin-set, wound-healing and related defects. *Potato biology and biotechnology: Advances and perspectives*, 471-500.
- Misener, G. C. (1994). Relationship between damage index and height loss of potatoes during storage. *Drying Technology*, 12(7), 1735-1741.
- Nguyen, T. A., Verboven, P., Scheerlinck, N., Vandewalle, S., & Nicolaï, B. M. (2006a). Estimation of effective diffusivity of pear tissue and cuticle by means of a numerical water diffusion model. *Journal of Food Engineering*, 72(1), 63-72.
- Nguyen, T. A., Dresselaers, T., Verboven, P., D'hallewin, G., Culeddu, N., Van Hecke, P., & Nicolaï, B. M. (2006b). Finite element modelling and MRI validation of 3D transient water profiles in pears during postharvest storage. *Journal of the Science of Food and Agriculture*, 86(5), 745-756.
- Nguyen, T. A., Verboven, P., Schenk, A., & Nicolaï, B. M. (2007). Prediction of water loss from pears (*Pyrus communis* cv. Conference) during controlled atmosphere storage as affected by relative humidity. *Journal of food engineering*, 83(2), 149-155.
- Öztürk, E., & Polat, T. (2016). The Effect of Long Term Storage on Physical and Chemical Properties of Potato. *Turk J Field Crops*, 21(2), 218-223.
- Panitkin, V. A., Dzikovich, K. A., Prokozhev, V. V., Treushnikova, N. A., Konotantinova, V. L., & Zhukov, S. N. (1979). Effect of different forms and doses of potassium fertilizer on change in potato quality during storage. *Agrokimiya*, 9(1979), 30-36.
- Park, Y. M. (1991). Fruit resistance to gas diffusion of mature McIntosh apples in relation to lenticel anatomy. *Journal of the Korean Society for Horticulture Science*, 32, 478-483.
- Peters, J. & Wiltshire, J. (2006). Preserving potato skin finish during storage. British Potato Council
- Pinhero, R. G., Coffin, R., & Yada, R. Y. (2009). Post-harvest storage of potatoes. *Advances in potato chemistry and technology*. Academic, New York, 339-370.

- Popenoe, H., King, S. R., Leon, J., & Kalinowski, L. S. (1989). Lost crops of the Incas. Little-known plants of the Andes with promise for worldwide cultivation. National Academy Press, Washington, 139-161
- Rady, A. M., & Soliman, N. (2013). Evaluation of surface effect, on mechanical damage of potato tubers using different methods. In 2013 Kansas City, Missouri, July 21-July 24, 2013 (p. 1). American Society of Agricultural and Biological Engineers.
- Riederer, M., & Muller, C. (Eds.). (2008). Annual Plant Reviews, Biology of the Plant Cuticle (Vol. 23). John Wiley & Sons.
- Riederer, M., & Schreiber, L. (2001). Protecting against water loss: analysis of the barrier properties of plant cuticles. *Journal of experimental botany*, 52(363), 2023-2032.
- Sabba, R. P., & Lulai, E. C. (2002). Histological analysis of the maturation of native and wound periderm in potato (*Solanum tuberosum* L.) tuber. *Annals of Botany*, 90(1), 1-10.
- Sawyer, R. L., & Dallyn, S. L. (1964). Internal sprouting of potatoes. *American Journal of Potato Research*, 41(2), 59-69.
- Schippers, P. A. (1971). The influence of curing conditions on weight loss of potatoes during storage. *American Potato Journal*, 48(8), 278-286.
- Schönherr, J., & Ziegler, H. (1980). Water permeability of *Betula* periderm. *Planta*, 147(4), 345-354.
- Schreiber, L., Franke, R., & Hartmann, K. (2005). Wax and suberin development of native and wound periderm of potato (*Solanum tuberosum* L.) and its relation to peridermal transpiration. *Planta*, 220(4), 520-530.
- Scott, R. I., Chard, J. M., Hocart, M. J., Lennard, J. H., & Graham, D. C. (1996). Penetration of potato tuber lenticels by bacteria in relation to biological control of blackleg disease. *Potato Research*, 39(3), 333-344.
- Secor, G. A., & Gudmestad, N. C. (1999). Managing fungal diseases of potato. *Canadian Journal of Plant Pathology*, 21(3), 213-221.
- Serra, O., Chatterjee, S., Figueras, M., Molinas, M., & Stark, R. E. (2014). Deconstructing a plant macromolecular assembly: chemical architecture, molecular flexibility, and mechanical performance of natural and engineered potato suberins. *Biomacromolecules*, 15(3), 799-811.
- Singh, B. N., & Mathur, P. B. (1937). Studies in potato storage: investigation of physiological and chemical changes during the development and ripening of potato tubers. *Annals of Applied Biology*, 24(3), 469-474.
- Singh, J., & Kaur, L. (Eds.). (2016). *Advances in potato chemistry and technology*. Academic press.
- Sparks, W. C. (1954). Effects of mechanical injury upon the storage losses of Russet Burbank potatoes.

Srikiatden, J., & Roberts, J. S. (2006). Measuring moisture diffusivity of potato and carrot (core and cortex) during convective hot air and isothermal drying. *Journal of Food Engineering*, 74(1), 143-152.

Srikiatden, J., & Roberts, J. S. (2008). Predicting moisture profiles in potato and carrot during convective hot air drying using isothermally measured effective diffusivity. *Journal of Food Engineering*, 84(4), 516-525.

UNECE Standard S-1 2016 edition concerning the certification and commercial quality control of seed potatoes

Veerman, A., & Wustman, R. (2005). Present state and future prospects of potato storage technology. *Potato in progress*. Wageningen Academic Publishers, Wageningen, 179-189.

Veraverbeke, E. A., Van Bruaene, N., Van Oostveldt, P., & Nicolai, B. M. (2001). Non destructive analysis of the wax layer of apple (*Malus domestica* Borkh.) by means of confocal laser scanning microscopy. *Planta*, 213(4), 525-533.

Veraverbeke, E. A., Verboven, P., Scheerlinck, N., Hoang, M. L., & Nicolai, B. M. (2003). Determination of the diffusion coefficient of tissue, cuticle, cutin and wax of apple. *Journal of Food Engineering*, 58(3), 285-294.

Verboven, P., Kerckhofs, G., Mebatsion, H. K., Ho, Q. T., Temst, K., Wevers, M., Cloetens, P. & Nicolai, B. M. (2008). Three-dimensional gas exchange pathways in pome fruit characterized by synchrotron X-ray computed tomography. *Plant physiology*, 147(2), 518-527.

Vogt, E., Schönherr, J., & Schmidt, H. W. (1983). Water permeability of periderm membranes isolated enzymatically from potato tubers (*Solanum tuberosum* L.). *Planta*, 158(4), 294-301.

Welty, J. R., Wicks, C. E., Rorrer, G., & Wilson, R. E. (2009). Fundamentals of momentum, heat, and mass transfer. John Wiley & Sons.

Wilson, W. D., MacKinnon, I. M., & Jarvis, M. C. (2002). Transfer of heat and moisture during oven baking of potatoes. *Journal of the Science of Food and Agriculture*, 82(9), 1074-1079.

Xu, Y., & Burfoot, D. (1999). Simulating the bulk storage of foodstuffs. *Journal of food engineering*, 39(1), 23-29.

Xu, Y., Burfoot, D., & Huxtable, P. (2002). Improving the quality of stored potatoes using computer modelling. *Computers and electronics in agriculture*, 34(1), 159-171.

Appendices

Appendix A.	Membrane diffusion model
Appendix B.	3D moisture diffusion model
Appendix C.	Deciding on the air domain size for the 1D moisture diffusion model
Appendix D.	Deciding on the potato thickness in the 1D moisture diffusion model
Appendix E.	Deciding on the flow regime for the 3D moisture diffusion model
Appendix F.	Deciding on the air domain size for the 3D moisture diffusion model
Appendix G.	Results of the calibration experiment

Appendix A Membrane diffusion model

The following general formulas belong to the schematic overview described in Figure 1. N ($\frac{kg}{m^2s}$) is the flux of water, C_i the concentration ($\frac{kg}{m^3}$) in the different phases or at the interfaces of the phases. C_m the concentrations on the interfaces in the membrane. The D 's are the diffusion coefficients ($\frac{m^2}{s}$). δ 's are the thicknesses of the stagnant film layers (m). L is the thickness of the membrane (m).

$$N = -\frac{D_R}{\delta_R}(C_{Ri} - C_R)$$

$$N = -\frac{D_P}{\delta_P}(C_P^g - C_{Pi}^g)$$

$$N = -\frac{D_M}{L}(C_{Pm} - C_{Rm})$$

Forced convection takes place on the outside of the potato in the air phase. The mass and heat convection formulas are coupled. A constant distribution of water among the potato is assumed. With this assumption only the skin is rate limiting for the flux and not the moisture conductivity within the potato this model.

The general flux equation is used (Janssen, 2014):

$$N = -kov(C_p^g - C_R)$$

The diffusion of water inside the potato is neglected, as the potato is seen as a homogeneous solid without a boundary layer. The concentration of water in the potato can be calculated using the moisture content, volume and weight of the potato sample. The moisture content of the air is calculated as the absolute humidity (AH). The relative humidity (RH) is determined as the ratio of water vapour pressure over the saturated vapour pressure (P_{sat}). The water vapour pressure can be calculated when the relative humidity and saturated vapour pressure are known. Data is known for 2 storage seasons for the Miss Malina variety. The known data is product and air temperature (T), relative humidity, ventilation and weight loss data. All acquired in a commercial storage facility.

The saturated vapour pressure is temperature dependent and can be calculated with the Buck equation (Buck Research Manual (1996)). This can be used in the general law of perfect gases resulting in the absolute humidity, which is the water concentration in the air.

$$P_w = P_{sat} * 1000 * \frac{RH}{100} [Pa]$$

$$P_{sat} = 0.61121e^{(18.678 - \frac{T}{234.5})(\frac{T}{257.14 + T})}, \quad T = [^{\circ}C], \quad P_{sat} = [kPa] \text{ (Buck equation, 1981)}$$

$$AH = \frac{P_w}{RT}, \quad T = [K]$$

$$AH = \frac{0.61121e^{(18.678 - \frac{T}{234.5})(\frac{T}{257.14 + T})} * 10 * RH * MW_w}{R(T + 273.15)} \left[\frac{kg}{m^3} \right], \quad T = [^{\circ}C]$$

Where MW_w is the molecular weight of water ($\frac{kg}{mol}$).

The convective mass transfer coefficient, the flux and the driving forces are known. The skin mass transfer coefficient can be calculated.

The concentration of water in the potatoes is calculated using the commercial storage data with:

$$C_w = \frac{(M_{air} - M_{UWW})}{V} \left[\frac{kg}{m^3} \right]$$

In which V is the volume of the potatoes (m^3)

The flux of water to the environment is calculated with:

$$N = \frac{\frac{\Delta M}{\Delta t}}{A}$$

In which A is the surface area of the potatoes (m^2)

Or the general flux equation:

$$N = -kov * (C_w - AH) \left[\frac{kg}{m^2s} \right], \quad T = [^{\circ}C]$$

With:

$$kov = \left(\frac{1}{k_{skin}} + \frac{1}{k_{air}} \right)^{-1}$$

Resulting in:

$$\frac{\frac{\Delta M}{\Delta t}}{opp(M_{data})} = - \left(\frac{1}{k_{skin}} + \frac{1}{k_{air}} \right)^{-1} (C_w - AH)$$

In which

$$k_{skin} = \frac{-N * k_{air}}{k_{air}(t)(C_w - AH) + N} \left[\frac{m}{s} \right]$$

k_{air} is the contribution of the external boundary layer ($m s^{-1}$). And can be calculated with the following functions (Nguyen et al., 2007) based on low velocity forced convection within a packed bed of spheres equations (Bird et al., 2007).

$$\frac{1}{k_{air}} = \frac{h_m V_w}{RT} \rho_{sat}$$

$$h_m = \frac{h_T}{\rho_a c_p Le^{\frac{2}{3}}}$$

$$h_T = \frac{\lambda Nu}{D_p}$$

$$Nu = 0.364 * Re^{0.558} * Pr^{\frac{1}{3}} \quad (Minh et al., 1969)$$

$$k_{air} = \frac{RT(t)}{0.364 \rho_{sat(T)}^{1.558} v_0^{0.558} D_p^{-0.442} (1 - \epsilon)^{-0.558} \phi^{0.558} \mu^{\left(\frac{1}{3} - 0.558\right)} \rho_a^{-\frac{1}{3}} D_a^{\frac{2}{3}} V_w}$$

With:

$$\mu = 1.458 * 10^{-6} * \frac{(T + 273.15)^{\frac{3}{2}}}{T + 273.15 + 110.4} \text{ (Sutherland's law, 1983)}$$

ρ_{sat} is the saturated vapour density ($kg\ m^{-3}$), D_p is the diameter of the potato (m), λ is the thermal conductivity of air ($Wm^{-1}K^{-1}$), ρ_a the air density ($kg\ m^{-3}$), D_a the water vapour diffusivity (m^2s^{-1}), v_0 the superficial velocity of air (ms^{-1}), μ the dynamic viscosity of air ($kgm^{-1}s^{-1}$), c_p the heat capacity of air ($Jkg^{-1}K^{-1}$), ϵ the potato bulk porosity (0.4 according to Xu et al., 2002) and ϕ the shape factor of the potatoes (based on hand measured potato data).

The shape factor is defined as the mean ratio between the volume of the potato and the volume of a sphere equal in diameter to the smallest dimension of the potato (Wilson et al., 2002). This will correct the spherical functions for the irregular shape of the potato.

Appendix B 3D moisture diffusion model

The 3D moisture diffusion model was made in a few steps. For the first step a temperature model of both domains is made. For the air domain:

$$\rho_a c_{p_a} * \frac{\partial T_a}{\partial t} + \rho_a c_{p_a} u * \nabla T_a - k_a \nabla^2 T_a = 0, \quad \text{in } (0, T_a] \times \Omega_a$$

In which k_a is the thermal conductivity of air (W/mK)

This formula holds for temperatures greater than 0 and less or equal to T.

With the boundary conditions:

$$T_a = T_{a,in}, \quad \text{on } [0, T_a] \times \partial\Omega_{a1}$$

$$\frac{\partial T_a}{\partial x} = 0, \quad \text{on } [0, T_a] \times \partial\Omega_{a3,4}$$

$$\frac{\partial T_a}{\partial y} = 0, \quad \text{on } [0, T_a] \times \partial\Omega_{a2}$$

$$T_p = T_a, \quad \text{on } [0, T_a] \times \partial\Omega_p$$

And the initial condition:

$$T_a(0, j) = T_{a,0}, \quad \text{on } j \in \Omega_a$$

For the potato domain a similar temperature balance is used:

$$\rho_p c_{p_p} * \frac{\partial T_p}{\partial t} - k_p \nabla^2 T_p = 0, \quad \text{in } (0, T_a] \times \Omega_p$$

With the boundary condition:

$$T_p = T_a, \quad \text{on } [0, T_a] \times \partial\Omega_p$$

And the initial condition:

$$T_p(0, j) = T_{p,0}, \quad \text{on } j \in \Omega_p$$

For the water concentration in the air a balance was made:

$$\frac{\partial c_a}{\partial t} - \nabla D_a \nabla^2 c_a + u \nabla c_a = 0, \quad \text{in } (0, c_a] \times \Omega_a$$

With the following boundary conditions

$$c_a = c_{a,in} = \frac{RH_{in}(t) * \rho_{sat}(T) * 10}{RT_a}, \quad \text{on } [0, c_a] \times \partial\Omega_{a1}$$

$$\frac{\partial c_a}{\partial x} = 0, \quad \text{on } [0, c_a] \times \partial\Omega_{a3,4}$$

$$\frac{\partial c_a}{\partial y} = 0, \quad \text{on } [0, c_a] \times \partial\Omega_{a2}$$

$$kov(c_p - c_a) = D_a \nabla c_a - u c_a, \quad \text{on } [0, T_a] \times \partial\Omega_p$$

And the following initial condition:

$$c_a(0, j) = c_{a,0}, \quad \text{on } j \in \Omega_a$$

The water concentration balance for the potato:

$$\frac{\partial c_p}{\partial t} - \nabla D_p \nabla^2 c_p = 0, \quad \text{in } (0, c_a] \times \Omega_p$$

With the boundary conditions:

$$kov(c_a - c_p) = D_p \nabla c_p, \quad \text{on } [0, T_a] \times \partial\Omega_p$$

And the initial conditions:

$$c_p(0, j) = c_{p,0}, \quad \text{on } j \in \Omega_p$$

Around the potato is a laminar incompressible air flow where $u = \begin{pmatrix} u \\ w \\ z \end{pmatrix}$, a flow vector in each direction. This flow can be expressed in the following balance:

$$\rho_a \frac{\partial u}{\partial t} + \rho_a (u \nabla) u = \nabla [pI + \mu (\nabla u + (\nabla u)^T)] + (\rho - \rho_{ref}) g$$

With g as the gravitational acceleration (m/s^2), μ the dynamic viscosity ($kg/m s$), ρ_{ref} the reference density of the air as the reduced pressure is used, p the pressure (Pa), I the identity matrix.

With the boundary conditions:

$$\frac{\partial u}{\partial x} = 0, \quad \text{on } [0, u] \times \partial\Omega_{a3,4}$$

$$\frac{\partial u}{\partial y} = 0.115 * FanState, \quad \text{on } [0, u] \times \partial\Omega_{a1}$$

FanState represents the state of the fan, on (1) or off (0).

And initial conditions

$$u(0, j) = u_0, \quad \text{on } j \in \Omega a$$

Appendix C Deciding on the air domain size for the 1D moisture diffusion model

To determine the size of the air domain after resizing the potato the 2D representation was investigated. Surface wise no change was made in the domain sizes by taking a total domain size of 5, like used in Figure 4. However this was a 2D symmetrical images, so the volume ratio was not the same. As the limiting factor is often a saturated air domain the volume ratio becomes important. To determine the effect of taking the surface ratio instead of the volume ratio, a parameter sweep of the air size domain was performed. The simulations where run from day 42 till 49 using the sensor data and a kov of $1\text{E-}09$ m/s. The size of the potato domain was $1.2 * \pi$, the effect of the total domain size was investigated. The total domain size is defined as the potato domain + the air domain. As can be seen in Figure 16 the air domain size does not influence the outcome of the simulation.

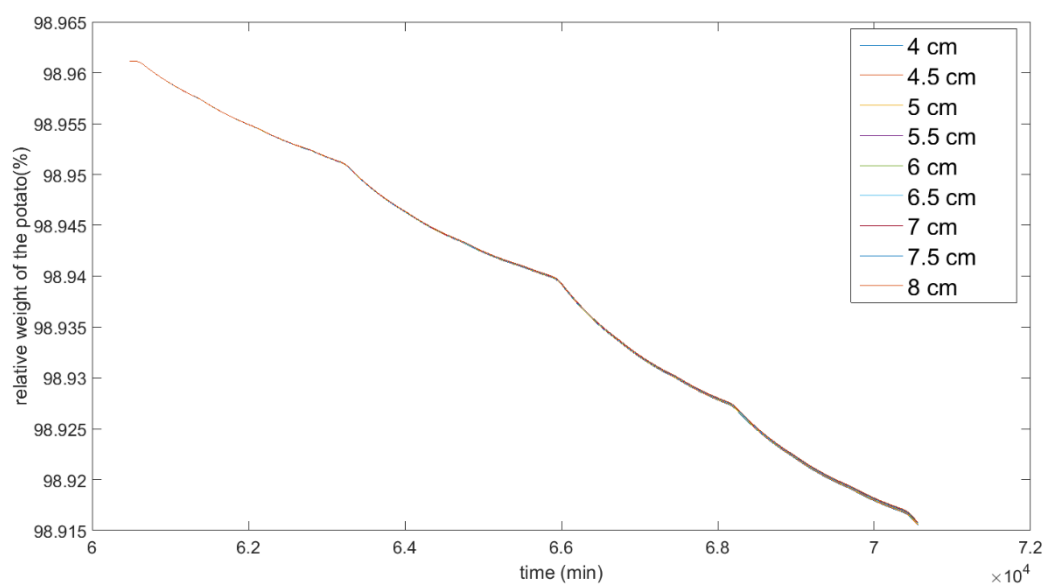


Figure 16 relative weight of the potato with different total domain sizes (potato domain size: 1.2π)

Appendix D Deciding on the potato thickness in the 1D moisture diffusion model

The standard setting of the thickness of the domains used within the heat transfer module of COMSOL multiphysics is 1 m. To determine the effect of this standard setting a simulation with the 1D moisture diffusion model was performed using the sensor data for day 42-49 of the standard simulations and a k_{ov} value of $1E-09$ m/s. As can be seen in Figure 17 the effect of changing this value is neglect able. Therefore the standard setting of 1 m is used in the rest of the experiments.

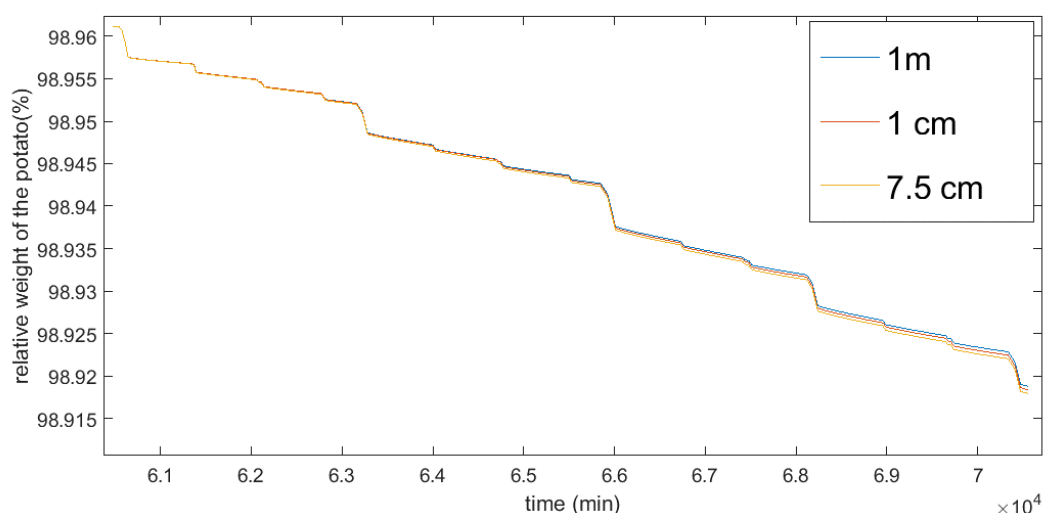


Figure 17 relative weight of the potato for different values of the potato thickness

Appendix E Deciding on the flow regime for the 3D moisture diffusion model

COMSOL has three main options within the single-phase flow: laminar flow, creeping flow and turbulent flow. This flow can be compressible, weakly compressible or incompressible. To determine which flow is best to use some simulations were performed. The simulations were 60 minute calculations in steps of 1 minute. The inflow of air switched on and off between 0 and 0.3 m/s every 10 minutes. Initial air temperature was 295 K, initial potato temperature 300 K. The incoming air had a temperature of 295 K and relative humidity of 95. The initial water concentration within the potato was 65500 mol/m³ (approximately 85% of the weight of the potato) and in the air 1000 mol/m³. Note: the concentration water in the air is physically impossible, it resembles a relative humidity of 104230% at room temperature (this error was made due to Kelvin Celsius conversions). As this mistake is used in all simulations the results are still useful, moreover the behaviour can still be checked. The potato was an ellipsoid with two radii of 4.8 cm and one of 7.5 cm. The air domain consisted of a cylinder with diameter 15 cm and height 15 cm. A μ of 1e-8 and D_p of 1e-6 were used. The D_c was 1e-9.

Compressible flow is the case when the Mach number is below 0.3. To reach this the local flow velocity needs to be below 100 m/s. This is obviously the case in this system. Therefore all 3 options are possible. In the table below the results of the tests can be found.

Table 5 results of different flow types and settings on calculation time, potato temperature, water concentration in the potato and maximum air velocity

Flow	type		Time (s)	T potato (K)	Concentration water potato (mol/m ³)	max air velocity (m/s)
Laminar		weakly	369	297.91	65243	0.39
		incompressible	206	297.95	65243	0.39
		compressible	212	297.3	65243	0.39
Turbulent	algebraicYplus	weakly	singularity reached			
	algebraicYplus	compressible	singularity reached			
	algebraicYplus	incompressible	671	297.77	65243	0.39
	k-e	incompressible	439	299.09	65243	0.39
	k-e	compressible	552	298.58	65243	0.39
	k-e	weakly	1073	299.28	65243	0.39
	spalart	incompressible	1071	297.93	65243	0.39
	L-Vel	incompressible	801	297.94	65243	0.39
Creeping		weakly	154	298.04	65243	0.50
		incompressible	106	298.08	65243	0.52
		compressible	60	297.48	65243	0.56

As can be seen in the table the compressible creeping flow has the lowest calculation time. However the laminar flow and turbulent flow show the same max air speed and also same flow profile (see Figure 18, Figure 19 & Figure 20 and Figure 21 & Figure 22). As it was known that turbulent flow would require more calculation time but is the most realistic it was performed to test which flow (creeping or laminar) resembled turbulent flow the most. Air is compressible, however the density

does not change much in the temperature ranges of the study therefore incompressible was also tested. Out of this it can be concluded that laminar incompressible flow is the best scenario and will be used in the rest of this study.

Recommendations: when continuing with the 3D model: check what if the potato is not in the middle of the air domain, as normally also other potatoes who “block” a side. A test can also be performed with multiple potatoes within the simulation. Or use other shape air domain, instead of a perfect cylinder. The turbulent behaviour can completely change when more objects are interfering with the flow.

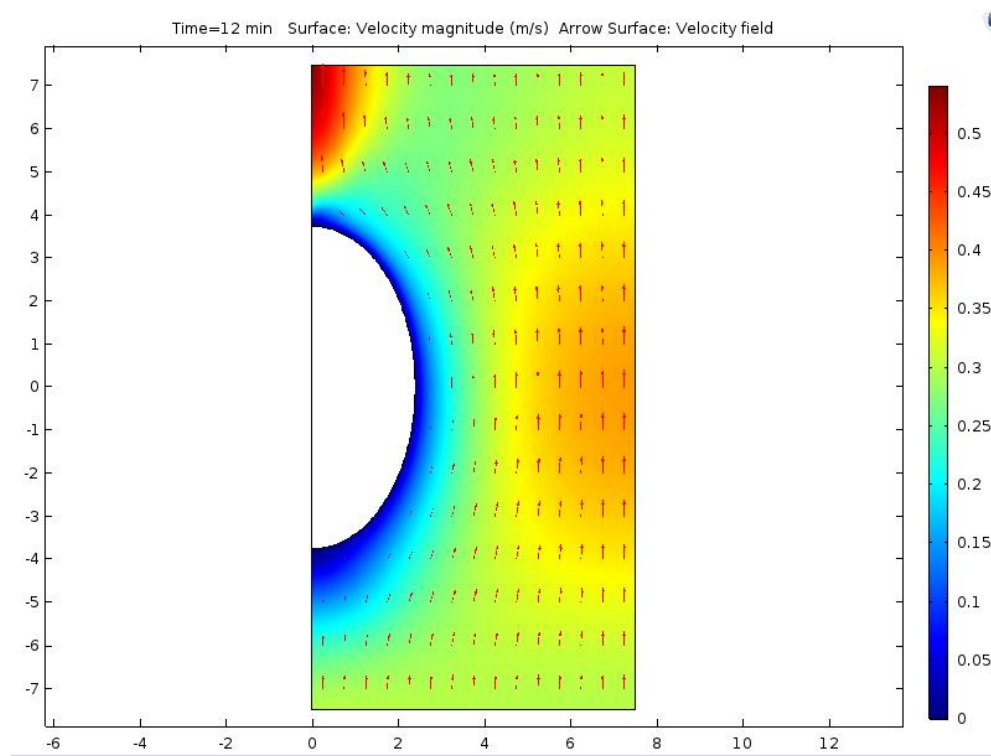


Figure 18 Creeping compressible flow (incompressible and weakly compressible looked the same)

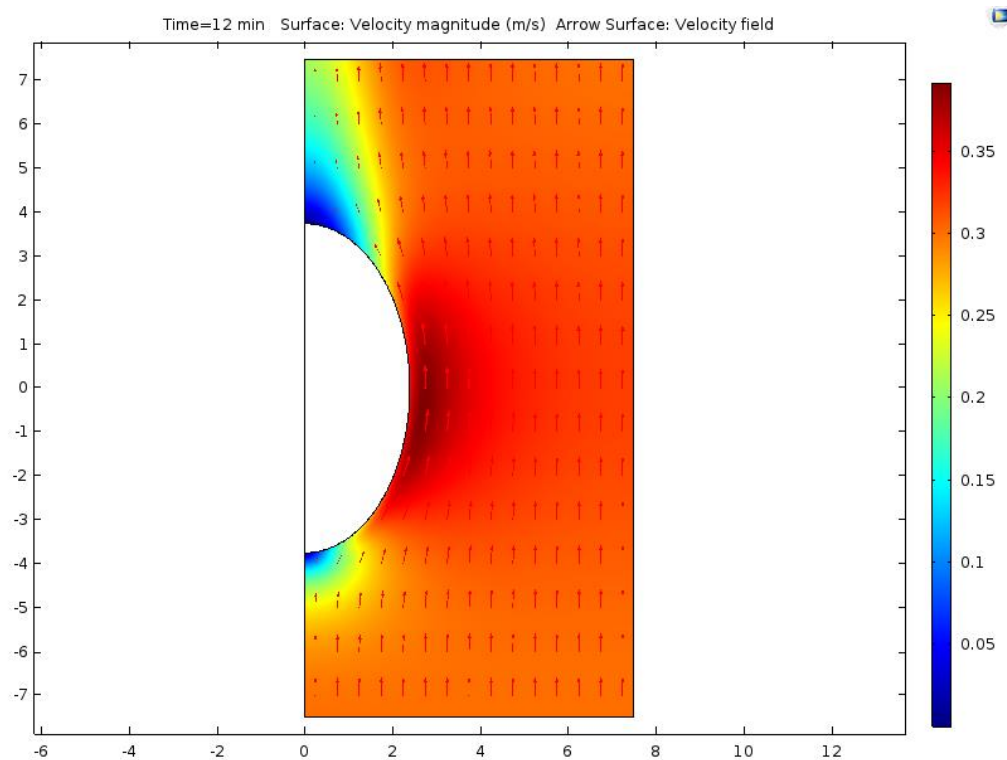


Figure 19 Turbulent k-e compressible flow

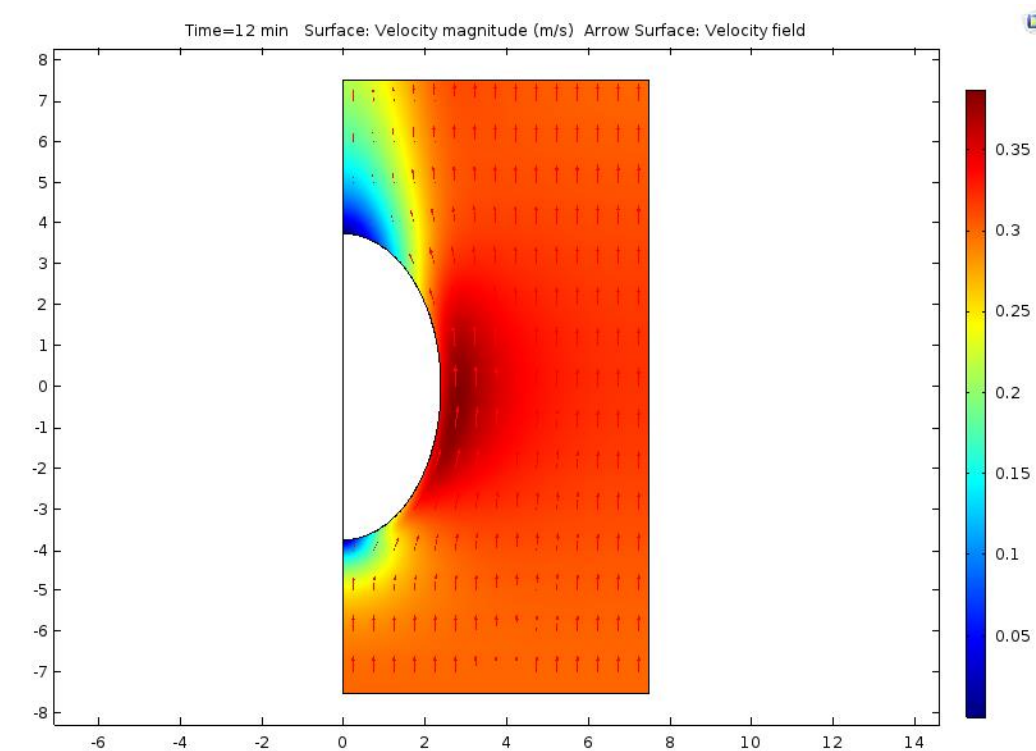


Figure 20 Turbulent k-e incompressible flow

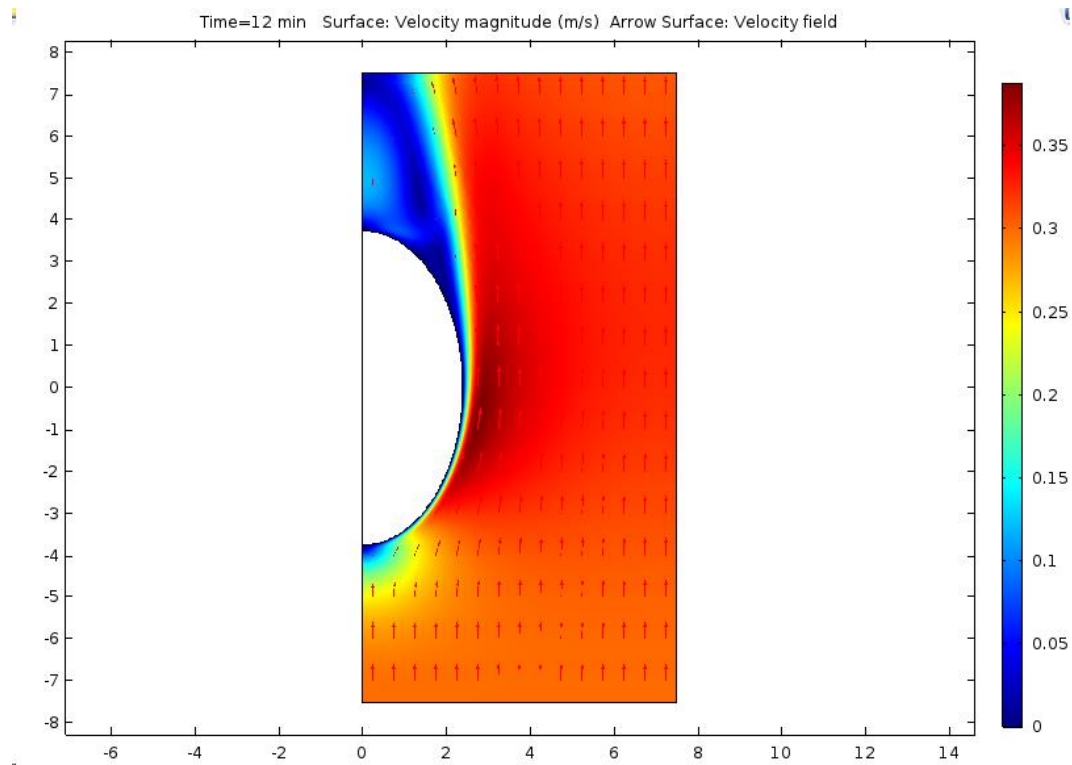


Figure 21 Turbulent y-plus incompressible flow (spalart & L-Vel showed a similar result)

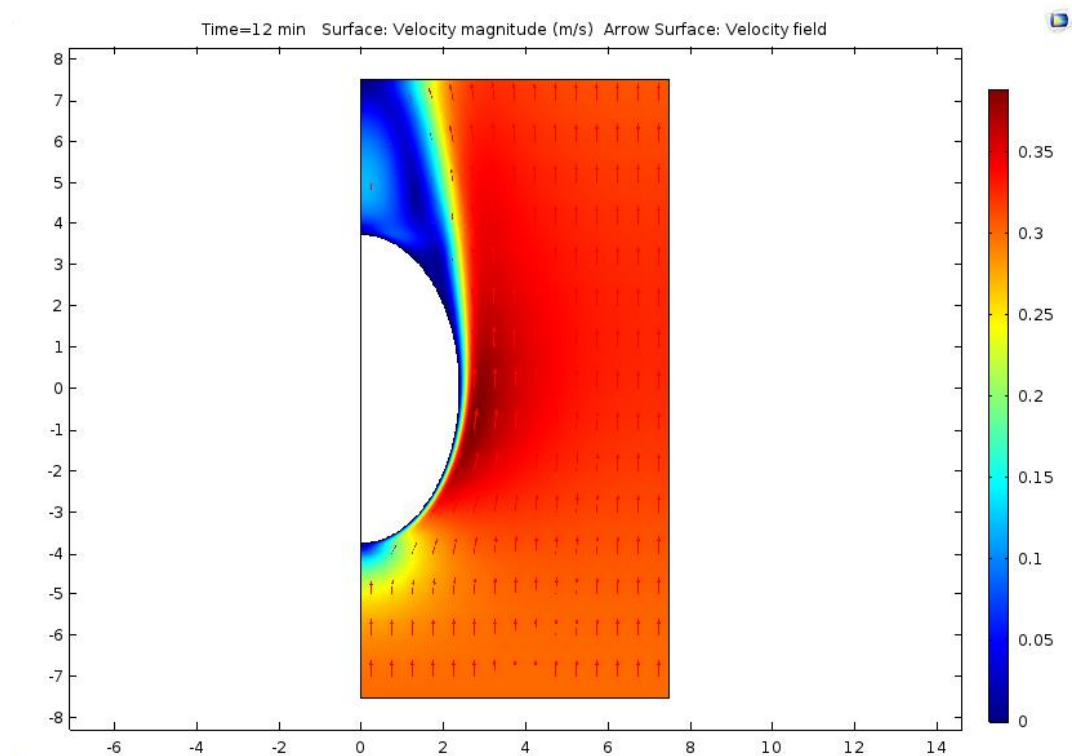


Figure 22 laminar incompressible flow

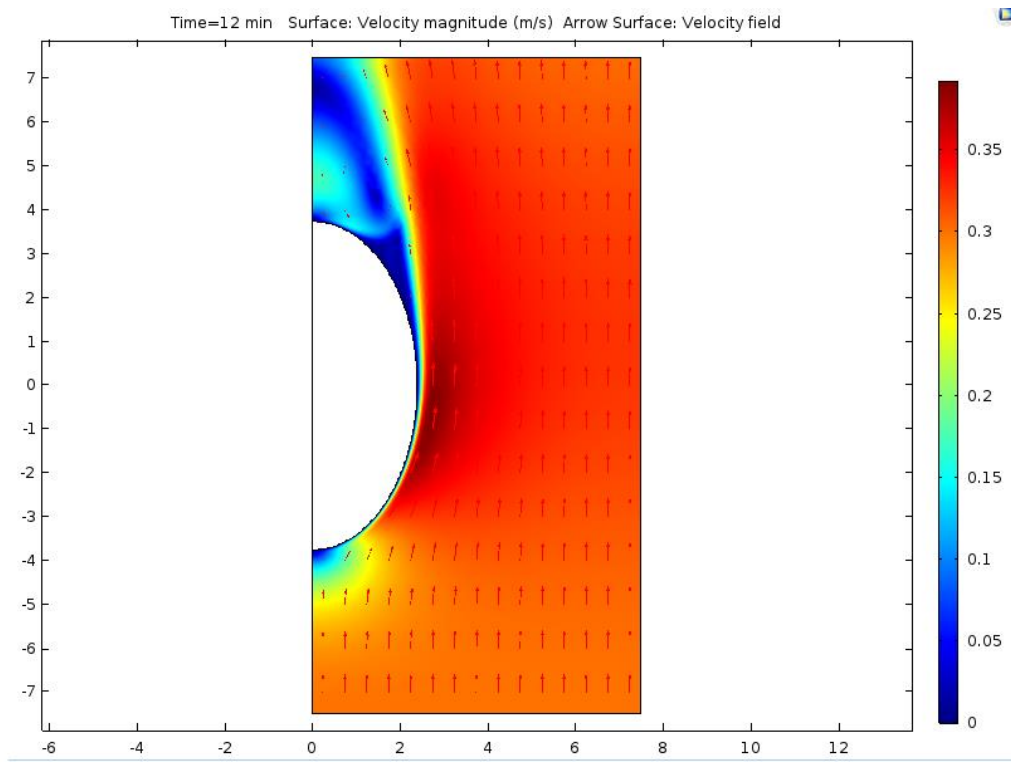


Figure 23 laminar compressible flow

Appendix F Deciding on the air domain size for the 3D moisture diffusion model

To determine which dimensions of the air domain is best to use some simulations were performed. The simulations were 60 minute calculations in steps of 1 minute. The inflow of air switched on and off between 0 and 0.3 m/s every 10 minutes. Laminar incompressible flow was used. Initial air temperature was 295 K, initial potato temperature 300 K. The incoming air had a temperature of 295 K and relative humidity of 95. The initial water concentration within the potato was 65500 mol/m³ (approximately 85% of the weight of the potato) and in the air 1000 mol/m³. Note: the concentration water in the air is physically impossible, it resembles a relative humidity of 104230% at room temperature (this error was made due to Kelvin Celsius conversions). As this mistake is used in all simulations the results are still useful, moreover the behaviour can still be checked. The potato was an ellipsoid with two radii of 4.8 cm (r, the rotational axis in COMSOL) and one (z) of 7.5 cm and is always in the middle of the air domain. A κ of 1e-8 and D_p of 1e-6 were used. The D_c was 1e-9.

The settings and results of the simulation can be seen below. The average air speed was later on added and therefore not performed for all the scenarios, likewise the bulk porosity (% air of total volume). The r axis is the rotational axis, the air domain will be a cylinder with radius r and height z.

Table 6 results of different potato and air domain sizes on calculation time, potato temperature, water concentration in the potato maximum and air velocity and the percentage of air within the total simulated domain.

r_air (cm)	z_air (cm)	r_pot (cm)	z_pot (cm)	Inflow velocity (m/s)	time (s)	T potato (K)	concentration water in potato (mol/m ³)	max air speed (m/s)	average air speed (m/s)	% air of total volume
15	15	4.8	7.5	0.3	206	297.95	65243	0.39		97%
10	10	4.8	7.5	0.3	214	298.07	65243	0.48		88%
8	8	4.8	7.5	0.3	195	297.97	65243	0.68		78%
5	7.6	4.8	7.5	0.3	173	297.44	65243	4.74	0.75	39%
4.81	7.51	4.8	7.5	0.3	terminated after 20 hours (21% calculated)					34%
4.8	7.5	4.8	7.5	0.3	Error: bigger relative residual than the tolerance.					33%
5	8	4.8	7.5	0.3	175	297.51	65243	4.75		42%
6	8	4.8	7.5	0.3	151	297.74	65243	0.95	0.46	60%
6	9	4.8	7.5	0.3	143	297.72	65243	0.94		64%
6	10	4.8	7.5	0.3	204	297.87	65243	0.94	0.37	68%
8	9	4.8	7.5	0.3	194	298.12	65243	0.56		80%
8	12	4.8	7.5	0.3	221	298.14	65243	0.52		85%
12	8	4.8	7.5	0.3	145	297.82	65243	0.68		90%
20	8	4.8	7.5	0.3	104	297.53	65243	0.68		96%
30	8	4.8	7.5	0.3	122	297.54	65243	0.68		98%
5	7.7	4.8	7.5	0.3	173	297.49	65243	4.72	0.72	40%
5	7.7	4.8	7.5	0.15	159	297.77	65243	2.56	0.36	40%
5	7.7	4.8	7.5	0.10	104	297.92	65243	1.79	0.24	40%
5	7.7	4.8	7.5	0.115	140	298.30	65243	2.03	0.267	40%

As can be seen in the table the fastest solution with the standard settings was with an air domain of 20 by 8. However this is 96% air. To make it more realistic aimed was to get a bulk porosity of 40% (Xu et al., 2002). This was obtained with an air domain of 5 by 7.7.

Next the incoming air speed was changed to get a realistic average air speed. In the commercial storage 100 m³ air per m³ potato is pumped through per hour when the fan is on. The storage was stacked till 4 m. With 0.11 m³/s per m² of the storage, resulting in an air speed of 0.11 m/s. With a bulk porosity of 40% the average air speed is 0.278 m/s. This was approximately reached using an incoming air speed of 0.115 m/s.

Recommendation: when continuing with the 3D model: check what if the potato is not in the middle of the air domain, as normally also other potatoes who “block” a side. A test can also be performed with multiple potatoes within the simulation. Or use other shape air domain, instead of a perfect cylinder.

Appendix G Results of the calibration experiment

In the table below the SSE of each week with each kov value can be seen. N.P. means this simulation was not performed, as results already showed the best value. Note that week 12 only consisted of 2.4 days as not more data was available.

Table 7 SSE of the kov calibration for the 1 slab simulations

kov	wk1	wk2	wk3	wk4	wk5	wk6	wk7	wk8	wk9	wk10	wk11	wk12
1.00E-10	62.6726	6.3446	12.0580	15.0304	7.9331	11.9881	13.8447	13.0381	13.5350	4.8459	12.8651	0.8743
1.78E-10	55.3079	5.7740	11.3996	14.6041	7.5516	11.5058	13.2725	12.8978	13.0310	4.7021	12.7012	0.8569
3.16E-10	43.4633	4.8669	10.2849	13.8628	6.9013	10.6772	12.288	12.6505	12.1632	4.4530	12.4129	0.8266
5.62E-10	26.3453	3.5936	8.4815	12.5975	5.8335	9.2955	10.6414	12.2175	10.7097	4.0312	11.9095	0.7750
1.00E-09	8.3053	2.4022	5.8181	10.5150	4.2146	7.1271	8.0420	11.4691	8.4079	3.3477	11.0435	0.6904
1.78E-09	15.1830	3.7038	2.8006	7.3391	2.2167	4.1812	4.4555	10.0692	5.2085	2.3135	9.4385	0.5626
3.16E-09	148.7641	16.7488	2.8932	3.3511	1.4673	1.7920	1.3193	7.9766	2.3339	1.1902	7.0819	0.4068
5.62E-09	759.9200	73.3900	19.9727	1.4669	9.1032	6.6977	6.2953	4.9855	6.0873	1.3269	3.9003	0.3552
1.00E-08	2.97E+03	277.7814	102.5485	14.3988	50.0711	43.7357	47.666	1.8642	40.5059	8.1823	1.2503	0.9733
1.78E-08	N.P.	N.P.	N.P.	N.P.	N.P.	N.P.	N.P.	2.9848	188.0013	41.2443	5.6743	4.2725
3.16E-08	N.P.	N.P.	N.P.	N.P.	N.P.	N.P.	N.P.	25.4383	715.5862	165.7533	41.3901	17.0506
5.62E-08	N.P.	N.P.	N.P.	N.P.	N.P.	N.P.	N.P.	122.5529	2.45E+03	585.6773	182.8535	60.9802
1.00E-07	N.P.	N.P.	N.P.	N.P.	N.P.	N.P.	N.P.	471.0827	7.81E+03	1.94E+03	666.4525	202.2489

Table 8 SSE of the kov calibration for the 2 slab simulations

kov	wk1	wk2	wk3	wk4	wk5	wk6	wk7	wk8	wk9	wk10	wk11	wk12
1.00E-10	62.5322	19.3513	21.4237	7.7691	15.0865	12.9677	9.8925	5.8572	10.0901	1.7809	16.9271	1.3637
1.78E-10	55.1749	18.1337	20.5550	7.4742	14.5317	12.4679	9.4192	5.7678	9.6537	1.7260	16.7390	1.3406
3.16E-10	43.3435	16.0765	19.0667	6.9665	13.5733	11.6083	8.6106	5.6109	8.9061	1.6352	16.4075	1.3003
5.62E-10	26.2520	12.7595	16.6012	6.1166	11.9580	10.1713	7.2767	5.3387	7.6662	1.4946	15.8274	1.2308
1.00E-09	8.2558	7.9379	12.7595	4.7719	9.3664	7.9048	5.2327	4.8759	5.7441	1.3109	14.8251	1.1145
1.78E-09	15.2139	2.7196	7.6418	2.9063	5.6409	4.7844	2.6329	4.0388	3.2190	1.1925	12.9523	0.9302

3.16E-09	148.9550	4.3017	4.0286	1.2425	1.7417	2.0786	1.2856	2.8802	1.5419	1.6682	10.1483	0.6741
5.62E-09	760.4357	40.7028	14.5512	3.4790	3.8862	6.4301	9.3839	1.5326	7.4179	4.6281	6.1813	0.4444
1.00E-08	2973.1000	209.5034	85.5844	23.6843	35.2194	42.4860	56.2675	1.2997	45.5872	16.4690	2.1509	0.7463
1.78E-08	10172.0000	830.2249	370.3872	109.8769	176.5313	194.4968	240.6709	7.4965	199.6853	58.3777	4.1496	3.4880
3.16E-08	3.1829E+04	2.8715E+03	1.3450E+03	4.1676E+02	6.8691E+02	7.3439E+02	879.4423	38.8720	738.8100	198.5585	35.6146	15.2792
5.62E-08	9.1645E+04	9.1677E+03	4.3715E+03	1.4206E+03	2.3536E+03	2.4988E+03	2.945E+03	151.0111	2.495E+03	645.7257	169.8877	57.4761
1.00E-07	2.3897E+05	2.7322E+04	1.3005E+04	4.4768E+03	7.4049E+03	7.9671E+03	9.342E+03	525.6985	7.890E+03	2.044E+03	637.1847	195.7411

Table 9 SSE of the kov calibration for the 4 slab simulations

kov	wk1	wk2	wk3	wk4	wk5	wk6	wk7	wk8	wk9	wk10	wk11	wk12
1.00E-10	62.6731	17.5195	18.7322	4.8283	9.5265	7.0477	5.1475	13.8425	20.8135	5.0025	18.8257	1.6411
1.78E-10	55.3075	16.3642	17.9170	4.6176	9.0957	6.6925	4.8511	13.6985	20.1994	4.8566	18.6277	1.6154
3.16E-10	43.4645	14.4178	16.5237	4.2597	8.3578	6.0899	4.3567	13.4447	19.1358	4.6039	18.2787	1.5703
5.62E-10	26.3445	11.2975	14.2267	3.6758	7.1342	5.1097	3.5813	13.0001	17.3341	4.1756	17.6674	1.4924
1.00E-09	8.3043	6.8230	10.6845	2.8037	5.2375	3.6544	2.5296	12.2312	14.4134	3.4806	16.6098	1.3610
1.78E-09	15.1830	2.2318	6.1000	1.7765	2.7392	1.9738	1.6915	10.7906	10.1138	2.4250	14.6283	1.1500
3.16E-09	148.7689	4.9078	3.4249	1.5979	1.1006	1.8650	3.5364	8.6303	5.2811	1.2638	11.6422	0.8464
5.62E-09	759.8386	43.2252	15.6021	6.4626	7.1854	10.7560	17.2009	5.5195	5.5605	1.3312	7.3547	0.5322
1.00E-08	2.9719E+03	215.3385	89.5247	31.2840	45.5009	54.8058	73.8971	2.1857	33.8102	8.0871	2.7591	0.6837
1.78E-08	1.0169E+04	841.4527	379.3133	125.5279	198.7647	220.8203	275.5136	2.9265	170.3657	40.8723	3.7566	3.1587
3.16E-08	3.1818E+04	2.8922E+03	1.3635E+03	4.4625E+02	7.2996E+02	7.8499E+02	944.1659	24.6936	678.5707	164.8764	33.4430	14.4735
5.62E-08	9.1626E+04	9.2023E+03	4.4061E+03	1.4733E+03	2.4319E+03	2.5906E+03	3.0604E+03	120.5900	2.3808E+03	583.7289	164.6329	55.8200
1.00E-07	2.3893E+05	2.7361E+04	1.3003E+04	4.5663E+03	7.5400E+03	8.1267E+03	9.5290E+03	466.8188	7.6823E+03	1.8995E+03	626.4436	192.5640

Table 10 SSE of the kov calibration for the 12 slab simulations

kov	wk1	wk2	wk3	wk4	wk5	wk6	wk7	wk8	wk9	wk10	wk11	wk12
1.00E-10	62.6731	16.9132	17.8412	4.2204	19.9873	15.9981	11.6140	6.1497	10.1842	1.6161	15.5091	1.0853
1.78E-10	55.3086	15.7785	17.0447	4.0356	19.3482	15.4441	11.0956	6.0573	9.7463	1.5719	15.3291	1.0654
3.16E-10	43.4644	13.8687	15.6845	3.7237	18.2399	14.4881	10.2067	5.8953	8.9960	1.4998	15.0120	1.0307
5.62E-10	26.3444	10.8133	13.4461	3.2216	16.3582	12.8798	8.7300	5.6139	7.7510	1.3927	14.4575	0.9714
1.00E-09	8.3064	6.4543	10.0084	2.4946	13.2920	10.3086	6.4322	5.1347	5.8198	1.2682	13.5007	0.8730
1.78E-09	15.1832	2.0703	5.6100	1.7253	8.6142	6.6468	3.3807	4.2653	3.2778	1.2584	11.7173	0.7207
3.16E-09	148.7441	5.1107	3.2631	2.0030	3.2778	2.9596	1.2125	3.0528	1.5682	1.9231	9.0622	0.5212
5.62E-09	759.9468	44.0712	16.0213	7.6803	2.7672	5.5895	7.8703	1.6099	7.3780	5.2148	5.3560	0.3921
1.00E-08	2.9719E+03	217.3148	90.9665	33.9338	29.4839	38.5825	52.1872	1.2074	45.4051	17.6787	1.7813	0.8718
1.78E-08	1.0169E+04	845.4098	382.5424	130.6953	162.6337	185.1349	232.0041	7.1000	199.1775	60.5600	4.5732	3.9253
3.16E-08	3.1822E+04	2.8995E+03	1.3689E+03	4.5581E+02	6.5802E+02	7.1528E+02	8.6254E+02	3.7922E+01	737.4848	2.0249E+02	3.7405E+01	16.2632
5.62E-08	9.1638E+04	9.2218E+03	4.4176E+03	1.4905E+03	2.2992E+03	2.4623E+03	2.9131E+03	1.4907E+02	2.4917E+03	6.5252E+02	1.7392E+02	5.9403E+01
1.00E-07	2.3892E+05	2.7390E+04	1.3045E+04	4.5959E+03	7.3067E+03	7.8992E+03	9.2832E+03	5.2185E+02	7.8809E+03	2.0213E+03	6.4483E+02	1.9925E+02